Final Report

October / 2025

Student Project No. SF/TF 170/a

Title: Understanding the control of perpetual flowering and continuous runnering in strawberry

Dissecting the control of continuous cropping in strawberry

Camila Gonzalez[1'2]

[1] NIAB East Malling, New Rd, East Malling, West Malling ME19 6BJ

[2] University of Reading, School of Agriculture, Policy and Development, Reading RG6 7EU, UK

Supervisors:

Prof. Timo Hytönen[1'3]

Dr. Matthew Ordidge[2]

Prof. Daniel James Sargent

[1] NIAB East Malling, New Rd, East Malling, West Malling ME19 6BJ

[2] University of Reading, School of Agriculture, Policy and Development, Reading RG6 7EU, UK

[3] Department of Agricultural Sciences, Viikki Plant Science Centre, University of Helsinki, 00014 Helsinki, Finland

Report No: 4

This is the final report of a PhD project that ran from October 2021 to October 2025. The work was funded by AHDB, BBSRC and Berry Gardens

Reference herein to trade names and proprietary products without stating that they are protected does not imply that they may be regarded as unprotected and thus free for general use. No endorsement of named products is intended, nor is any criticism implied of other alternative, but unnamed, products.

CONTENTS

1. INDUSTRY SUMMARY 4
2. INTRODUCTION 5
3. MATERIALS AND METHODS 6
3.1. Plant material and growth conditions 6
3.2. GBS library preparation and sequencing 7
3.3. Genetic linkage map construction and imputation 8
3.4. Identification of candidate genes and gene expression analysis 9
3.5. Guide (gRNA) selection 9
3.6. Construction of sgRNA and CRISPR/Cas9 expression vectors 10
3.7. Cloning 11
3.8. *Agrobacterium*-mediated transformation and plant regeneration 11
3.9. Screening of mutant lines 12
3.10. Phenotyping of mutant lines 12
3.11. Statistical analysis 12
4. RESULTS 14
5. DISCUSSION 36
5.1. Understanding the control of perpetual flowering in strawberry 37
5.2. Dissecting the control of continuous runnering in strawberry 39
5.3. Study limitations 41
5.4. Future directions and concluding remarks 43
6. REFERENCES 46

1. Industry Summary

Consumer demand for year-round strawberry fruit has increased the need to extend the cropping season. Perpetual flowering cultivars, which produce fruit continuously throughout the growing season, offer a promising solution. However, these cultivars typically exhibit reduced runner production, due to a genetic trade-off between flowering and runnering, presenting challenges for propagation and breeding efforts. Additionally, limited understanding of the mechanisms controlling these traits in the cultivated strawberry (*Fragaria* × *ananassa*) has hindered the application of advanced breeding or crop improvement tools. This PhD work aimed to better understand the genetic and molecular mechanisms underlying perpetual flowering and continuous runnering in strawberry, to contribute to the development of perpetual flowering cultivars with extended fruiting periods and improved propagation potential.

In this work, the control of perpetual flowering was explored by functionally studying key flowering genes *TFL1* and *FT1* in *F. x ananassa* seasonal flowering cultivar 'Malling Centenary' and perpetual flowering cultivar 'Calypso' using CRISPR/Cas9 genome editing and phenotyping. *FaTFL1* mutant lines exhibited early flowering and reduced runner production under long day conditions, validating its role as a floral repressor and demonstrating the regulatory link between these traits. *FaFT1* mutant lines presented alteration in floral and fruit morphology suggesting its role in floral development. Furthermore, the genetic regulation of the trade-off between flowering and runnering was studied through genotyping-by-sequencing based QTL mapping using a woodland strawberry (*Fragaria vesca*) F_2 mapping population developed from a cross between an ecotype from Spain with continuous runnering habit and an accession from Iceland with a 'normal' runnering habit. Two additive QTLs associated with continuous runnering were identified using interval mapping. The most significant QTL was narrowed and validated using cleave amplified polymorphic sequences (CAPS) for genotyping in a second validation population. Candidate genes associated with dormancy and axillary bud outgrowth were identified in both QTLs. Gene expression analysis showed a significant downregulation of two candidate genes in continuous runnering individuals supporting their role in the control of this trait. Finally, the functional role of the two main candidate genes for continuous runnering was explored through CRISPR/Cas9 targeted mutagenesis. Two mutant lines for one of the main candidate genes were obtained, however the editing efficiency was very low and consequently this part of the study was not pursued to completion. The work developed within this thesis provides valuable insight into the mechanisms controlling perpetual flowering and the developmental trade-off between generative and vegetative reproduction that could inform future crop improvement strategies.

2. Introduction

Consumer demand for year-round strawberry availability, combined with rising transportation costs for imported fruit, has increased the need to extend the strawberry cropping season. This objective has become a key focus of strawberry breeding programs worldwide. Perpetual flowering cultivars, which produce fruit throughout the growing season, present a promising solution. While selective breeding has successfully developed such varieties, a deeper understanding of the genetic mechanisms controlling this trait in cultivated strawberry could further optimize flowering time, extend harvest periods, and enhance annual yields.

However, perpetual flowering cultivars often produce fewer runners due to a genetic trade-off between flowering and vegetative propagation. This reduction in runnering affects future production and breeding efforts. The limited understanding of the genetic and molecular mechanisms underlying perpetual flowering and runnering in the cultivated strawberry has hindered the full exploitation of these traits through advanced breeding tools such as marker-assisted selection and genome editing. Developing a more comprehensive understanding of these genetic pathways could accelerate the production of improved strawberry cultivars with extended fruiting periods, optimized yields, and efficient propagation potential.

Therefore, the broad aim of this study was to advance the understanding of the genetic regulation of perpetual flowering and the flowering-runnering trade-off in strawberry. To achieve this, this study had three objectives:

(1) Study the role of key flowering genes in the cultivated strawberry through genome editing
(2) Identify candidate genes influencing trade-off between flowering and runnering in the woodland strawberry by using QTL mapping and gene expression analysis
(3) Study the role of candidate genes through genome editing

Each research objective contributes to a deeper understanding of the genetic mechanisms controlling key reproductive traits in strawberry and offer insights for future breeding strategies, particularly regarding the use of genome editing technologies to improve important agronomical traits in the cultivated strawberry.

3. Materials and methods

3.1. Plant material and growth conditions

Objective 1: The *F. x ananassa* seasonal flowering 'Malling Centenary' and perpetual flowering 'Calypso' cultivars were used for this study. Stock material for genetic transformation was developed by sub-culturing *In vitro* shoots on Shoot Propagation Media (SPM) every 4-5 weeks. All *in vitro* plant material was maintained in a growth room under 20°C with a 16h light and 8h dark photoperiod provided by LED lamps (light output: 168-210 µmol/m²/s). Selected edited and wild-type (WT) lines were acclimatized to growth room conditions by transferring to a propagator with vermiculite for four weeks under the same *in vitro* growth conditions described previously. After acclimatization, plantlets were potted in compost and grown in a growth room under the following long day growth conditions: 18°C with a 16h light / 8h dark photoperiod. Light was provided by LED lamps (light output: 120 µmol/ m²/s red, 20 µmol /m²/s green, 20 µmol/m²/s blue, 20 µmol/m²/s far red).

Objective 2: An F_2 mapping population of 555 individuals was developed from a cross between *F. vesca* ES12 and ICE12 ecotypes. The parental lines were clonally propagated to develop 30 replicates per genotype. Both the mapping population and parents were phenotyped under controlled conditions at the University of Helsinki, Finland. For QTL validation, a second F_2 population of 120 individuals from the same cross was established and phenotyped at the National Institute of Agricultural Botany (NIAB) in East Malling, Kent, UK. Phenotypic traits evaluated included runner count, leaf count during short day treatments, leaf count to flower and flowering time. To evaluate trait segregation and identify potential QTLs associated with continuous runnering, three separate phenotypic experiments were conducted.

Phenotypic traits evaluated included runner count, leaf count during short day treatments, leaf count to flower and flowering time. To evaluate trait segregation and identify potential QTLs associated with continuous runnering, three separate phenotypic experiments were conducted. Experiment 1 (E1) involved single clones of 555 individuals from the mapping population and was conducted under autumn, mild winter and spring conditions in a greenhouse. Experiment 2 (E2) was conducted using 171 individuals from the mapping population, each with three replicates, and included autumn, mild winter and spring seasonal treatments. Parental clones were also evaluated under the same experimental conditions; however, half of the plants were transferred to winter treatment after six weeks of autumn treatment, while the remaining plants were transferred directly to spring treatment. Experiment 3 (E3) involved single clones of 120 individuals from the validation population and included autumn and summer seasonal treatments.

Runner and leaf count observations were taken during short day treatments (autumn and winter) and consisted of weekly recording of new runners and leaves from the main crown. Leaf count to flower observations consisted of weekly recordings of new leaves produced from the main crown from the start of short day treatment (autumn) to the emergence of the first inflorescence. Flowering time was recorded as the number of days from the start of the long day treatment to the first open flower.

Objective 3: The *F. vesca* accession FIN56 was used in this study. To develop *in vitro* plant material for genetic transformation, plantlets were grown from seeds using the following protocol. A total of 20-30 seeds were cleaned with 75% ethanol for 1 minute and rinsed with sterile ultrapure water. Subsequently, surface sterilization was performed using a 1% NaClO solution with a few drops of Tween-20 for 5-10 minutes. Seeds were then washed four times with sterile ultrapure water and sown on plates containing H4 media without growth regulators. Seeds were germinated in a growth room at 20°C with a 16h light and 8h dark photoperiod provided by LED lamps (light output: 168-210 µmol/m²/s). After germination, seedlings were transferred to honey jars containing H4 with hormones and grown for four weeks before transformation.

3.2. GBS library preparation and sequencing

Objective 2: Genomic DNA for sequencing was extracted from young, freeze-dried strawberry leaves using the DNeasy® Plant Mini Kit (QIAGEN GmbH, Germany), following the manufacturer's instructions. For Cleaved Amplified Polymorphic Sequence (CAPS) marker genotyping, DNA was isolated using an in-house protocol. Briefly, leaf tissue was ground in extraction buffer containing 10% SDS, 1 M Tris-HCl, and 0.5 M EDTA. Afterwards, DNA was precipitated in isopropanol, washed with ethanol, and resuspended in AE buffer (QIAGEN GmbH, Germany). DNA concentration and quality was assessed using a NanoDrop™ 1000 Spectrophotometer and/or a Qubit® 2.0 Fluorometer.

Genomic DNA from the parents (ES12 and ICE12), F_1 hybrid and 90 individuals from the F_2 population were used to construct a genotyping-by-sequencing (GBS) library for QTL mapping. The 90 F_2 individuals comprised 22 continuous runnering lines and 68 lines showing cessation of runnering in SDs. The GBS library was prepared by restriction enzyme digestion of DNA samples with *ApeKI* (NEB, R0643), followed by ligation with barcode and common adapter sequences as described in the protocol by Elshire et al. (2011). A set of 96 different barcode sequences were used for labelling the samples. Barcoded samples were pooled and purified using the QIAquick PCR Purification Kit (QIAGENE GmbH, Germany)**,** according to the manufacturer's instructions. To obtain the final sequencing library, PCR amplification of the fragment pool with common adapter

primers was performed, and the PCR product was purified as described above. The fragment sizes and quality of the GBS library were checked through electrophoresis using a 1.5% TAE agarose gel and through a commercial quality control service (Novogene, UK).

3.3. Genetic linkage map construction and imputation

Objective 2: Genetic linkage mapping was performed using JoinMap 4.1 (Van Ooijen, 2006). Locus genotype frequencies and segregation distortion (Chi-square X^2) were calculated, and loci with significantly distorted segregation values (p-value < 0.005) were excluded from map construction. The interval mapping algorithm was used with an independence LOD score of 5.0 to group the markers and develop an initial genetic linkage map. To improve accuracy of QTL analysis, manual imputation of missing genotype data for each linkage group was carried out. For imputation, the genotype data was numerically ordered based on the physical position of the markers. Afterwards, a genetic linkage map was constructed using the imputed data and the regression mapping algorithm with an independence LOD score of 5.0. The marker distances were calculated in centimorgans (cM) according to the Haldane's mapping function. The final genetic linkage map graphs were generated using R/QTL (Broman et al., 2025).

The genetic linkage map genotype data and phenotypic data from the ES12xICE12 F_2 mapping population from Experiment 1 and 2 was used for QTL mapping. Analysis was performed by composite interval mapping using MapQTL ® 6.0 (Van Ooijen, 2004). The LOD significance threshold for the phenotypic traits were determined using a permutation test of 1000 iterations. The resulting genome wide significance threshold was applied to identify statistically significant QTLs. Whole genome and single chromosome QTLs scans were illustrated graphically using R/QTL.

CAPS markers for QTL validation and fine-mapping were developed based on the method described by Ruiz-Rojas et al. (2010). To design these markers, SNP variants at target loci were first identified using locus-specific sequence tags derived from parental GBS data. Subsequently genomic regions spanning ±1500 bp around each sequence tag were retrieved from the *Fragaria vesca* 'Hawaii-4' reference genome v4.0 using the JBrowse tool (Diesh et al., 2023) available through the Genome Database for Rosaceae (GDR) (Jung et al., 2019). Single-cut restriction enzyme recognition sites overlapping the SNPs were identified and PCR primers flanking the region containing the SNP were designed using Geneious Prime version 2023.1. CAPS markers were then validated using the genomic DNA from the parental lines and F_1 hybrid to confirm genotype specific restriction patterns. Genotyping was performed by PCR amplification using a touchdown protocol as described by Sargent et al. (2003). The resulting amplicons were digested with the appropriate restriction enzymes and resolved on a 1.5% TAE agarose gel.

QTLs were validated in 251 individuals from the F_2 mapping population and 120 individuals from the F_2 validation population by using CAPS markers flanking the QTL region. Genotype data was compared with phenotypic observation from Experiment 1-3 to determine QTL stability and reliability. For fine-mapping and identification of recombination points recombinant individuals were genotyped with additional CAPS markers located within the QTL.

3.4. Identification of candidate genes and gene expression analysis

Objective 2: To identify candidate genes associated with the continuous runnering trait, the gene annotation track within the QTL region, was extracted from the *Fragaria vesca* 'Hawaii-4' Genome v4.0 using JBrowse. Gene function prediction was performed by BLAST analysis using the Tripal MegaSearch tool from the Genome Database for Rosaceae (GDR). Potential candidate genes were then selected through manual curation based on their predicted functions.

For gene expression analysis, young leaf samples of selected individuals were frozen in liquid nitrogen and stored at -80°C before RNA extraction using an in-house method modified from Chang et al., (1993). Briefly, leaf tissue was ground in liquid nitrogen and RNA extraction buffer containing 3% CTAB, 2% PVP, 100 mM of Trish-HCL, 20 mM of EDTA, 1 M NaCl, 0.05%, Spermidine, and fresh β-Mercaptoethanol (1 %) was added to the buffer before use. Afterwards, RNA was isolated in chloroform, precipitated in LiCl (8 M), washed in 75% ethanol and resuspended in RNase-free water. RNA concentration and quality was assessed using a NanoDrop™ 1000 Spectrophotometer and/or a Qubit® 2.0 Fluorometer. cDNA synthesis was performed using 1 µg of RNA with the QuantiTect Reverse Transcription Kit (QIAGENE). Gene expression analysis was conducted in triplicate reactions via quantitative real-time PCR (RT-qPCR) using the SsoAdvanced Universal SYBR Green Supermix (Bio-Rad) and a CFX96/CFX384 real-time PCR detection system (Bio-Rad). Relative gene expression levels were calculated using the ΔΔCt (cycle threshold) method (Livak & Schmittgen, 2001), with *FvMSI1* (*Fragaria vesca* homologue of *MULTICOPY SUPPRESSOR OF IRA1*) as the normalization gene as described by (Mouhu et al., 2009).

3.5. Guide (gRNA) selection

Objective 1: Full-length sequences of the *F. x ananassa TFL1* (KR139762.1) and *FT1* (KR139759.1) homologues were used to identify CRISPR/Cas9 target sites using Geneious Prime 2023.1 (http://www.geneious.com/), CRISPOR (Haeussler et al., 2016), and CHOPCHOP (Labun et al., 2019). The selection of gRNA sequences was made to meet the following criteria: activity score Doench et al. (2016) between 0.5-1, specificity score Zhang et al. (2013) 50% or above, CG

content between 30-65%, gRNA self-folding free-energy between -2-0 kcal/mol, and the absence of potential off-targets with less than two mismatches.

Additionally, a BLAST search of the *FaTFL1* and *FaFT1* gene sequences was performed against the *F. x ananassa* cv. 'Royal Royce' v1.0 genome, and the resulting homoeologous and paralogous gene sequences were aligned to identify optimal target sites located specifically within conserved regions of the homoeologous gene copies. Potential off-targets were identified using both the *F.× ananassa* cv. 'Royal Royce' v1.0 and 'Camarosa' v1.0 genomes as reference sequences. All retrieved gene sequences were obtained from the Genome Database for Rosaceae (GDR) (Jung et al., 2019).

Objective 3: Complete gene sequences of *Fv5g35400.t1-t4* (8139 bp) and *Fv5g35401.t1-t2* (7586 bp) were used in this study. Gene sequence annotations were checked using the online tool GENESCAN (http://hollywood.mit.edu/GENSCAN.html). CRISPR/Cas9 target sites were identified using Geneious Prime 2023.1 (http://www.geneious.com/) and CRISPOR (Haeussler et al., 2016). The selection of gRNA sequences was made to meet the same criteria as objective 1. Potential off-targets were identified using *the F. vesca* Whole Genome v4.0.a2 reference genome (Shulaev et al., 2011). All retrieved gene sequences were obtained from the Genome Database for Rosaceae (GDR) (Jung et al., 2019).

3.6. Construction of sgRNA and CRISPR/Cas9 expression vectors

Objective 1 & 3: To develop CRISPR/Cas9 expression constructs, gRNA sequences targeting different exons of the genes of interest were paired to create single guide (sg)RNA vectors targeting dual sites. This design aimed to induce large deletions, thereby increasing the likelihood of effective gene disruption. For each gRNA, forward and reverse oligonucleotides with *BsaI* or *Esp3I* sticky ends were synthesized and annealed following the protocol by Decaestecker et al. (2019). The resulting gRNA1 and gRNA2 sequences were cloned into entry vectors EC54141 and EC54142, respectively. Final CRISPR/Cas9 expression constructs were assembled using the following components: EC15029 (pNos-KanR-tNos), EC54157 (p35S-SpCas9/P-IV2 intron-t35S), EC54141/EC54142 (pFVU6III-gRNA1/gRNA2-gRNA scaffold), and the backbone vector EC50507, using *BbsI-HF* restriction sites. All entry vectors used in this study were provided by Dr. Anindya Kundu (NIAB, Cambridge). Each construct included two sgRNAs under the control of the *F. vesca* U6III promoter, a CaMV 35S-driven SpCas9 nuclease gene containing a potato IV2 intron to suppress bacterial expression during cloning, and a kanamycin resistance gene for plant selection.

3.7. Cloning

Objective 1 & 3: All entry and expression constructs were assembled using Golden Gate cloning (Engler & Marillonnet, 2014). Vectors were transformed by heat-shock transformation using DH5α competent *E. coli* cells (Thermo Fisher Scientific). *E. coli* cell cultures were grown and plated on high salt LB broth/agar with antibiotics depending on the selection marker (100 µg/mL ampicillin, 100 µg/mL spectinomycin, 50 µg/mL kanamycin). Plasmids were isolated using the GeneJET Plasmid Miniprep kit (Thermo Fisher Scientific) and checked by restriction enzyme digestion and Sanger Sequencing using the Eurofins Genomics Mix2seq sequencing service.

3.8. *Agrobacterium*-mediated transformation and plant regeneration

Objective 1 & 3: *Agrobacterium*-mediated transformation was performed as described by Wilson et al. (2019) with minor modifications. The final CRISPR/Cas9 expression constructs were introduced into competent *Agrobacterium tumefaciens* strains EHA105 or AGL-1 (GoldBio) using a heat-shock method. Transformed cells were plated on low-salt LB agar containing 50 µg/mL kanamycin and rifampicin. Colonies harbouring the binary vector were cultured overnight in LB broth with the same antibiotics and pelleted at 2,000 × g for 10 minutes. The transformation inoculum was prepared by resuspending the pellet in *Agrobacterium* inoculum medium [filter-sterilized liquid MS-based media, glucose (30 g/L), Acetosyringone (100 µM), pH 5.2] to an optical density (OD600 nm) of 0.2-0.3. Leaflets were harvested from young expanding leaves of 4–5-week-old shoots and submerged in the inoculum. Explants for objective 1 were prepared by cutting the leaflets transversely with a scalpel to create 2 mm strips, while keeping the strips attached on one side of the leaf. Explants for objective 3 were prepared by cutting the petioles with a scalpel to create 1 cm pieces. Cut explants were incubated in the inoculum for 15 minutes and then blotted on sterile filter paper to remove excess inoculum. Explants were transferred to plates with Shoot Regeneration Media (SRM) and incubated in the dark for 4 days at 20°C. After dark incubation, explants were washed in a water solution with 400 mg/L of ticarcillin disodium/clavulanate potassium (TCA), blotted again on sterile filter paper, and transferred to SRM selection medium with TCA (400 mg/L) and kanamycin (50 mg/L) for selection. Explants were subcultured every 4-6 weeks, and shoots were harvested over a 6–8-month period. Harvested shoots were transferred to Strawberry Shoot Rooting Media (SSRM) or SPM and subcultured after two months to *Fragaria* Rooting Media (FRM). Control shoots (untransformed/azygous) were regenerated using the same method, but without co-cultivating the explants with the *Agrobacterium* inoculum, and the culture media did not contain antibiotics.

3.9. Screening of mutant lines

Objective 1 & 3: Leaf samples from regenerated shoots were collected and freeze-dried. Genomic DNA was extracted using the DNeasy Plant Kit (QIAGENE GmbH, Germany). Screening of transformed lines was initially done by PCR amplification of the pNos-KanR-tNos cassette from the expression vector. Screening of edited lines was performed using fragment analysis by capillary electrophoresis (CE). To do this, amplicons spanning the target regions were amplified using 6-FAM fluorescently labelled primers. Analysis was carried out at the John Innes Center using an ABI 3730 DNA Analyzer and a LIZ500 size standard. To further identify and characterize CRISPR/Cas9-induced edits in the screened lines, the Eurofins Genomics INVIEW CRISPR Check service was used. To prepare the amplicons for sequencing, the target site regions were amplified using Phusion High-Fidelity 2x PCR Master Mix (Thermo Scientific™) or Q5® High-Fidelity 2X Master Mix (New England Biolabs) with amplicon specific primers containing common sequencing adaptor overhangs (Forward: 5'-ACACTCTTTCCCTACACGACGCTCTTCCGATCT-3', Reverse: 5'-GACTGGAGTTCAGACGTGTGCTCTTCCGATCT-3'). Amplicons containing adapter sequences were purified using the QIAquick PCR Purification Kit (QIAGENE GmbH, Germany) or the Wizard® SV Gel and PCR Clean-Up System (Promega, UK).

3.10. Phenotyping of mutant lines

Objective 1: Primary T0 mutant and WT plants were propagated by runners to generate 5-10 clonal replicates per line, which were then used for phenotypic assessments. To investigate the phenotypic effect of CRISPR/Cas9 induced mutations in mutant lines, the following observations were recorded per plant under long day conditions: (1) flowering time (number of days from propagation to the first open flower), (2) total number of inflorescences, (3) total number of flowers per plant, (4) number of flowers per inflorescence (total number of flowers/total number of inflorescences), and (5) total number of runners. Observations were recorded for a period of five months.

3.11. Statistical analysis

Objective 1: All statistical analyses were performed using R-Studio version 2024.12.0. Before analysis, phenotypic data were checked for normality and homogeneity using the Shapiro-Wilk and Levene's test. For phenotypic trait comparisons, a one-way analysis of variance (ANOVA) was conducted to assess significant differences within experimental groups, followed by post hoc Tukey's HSD test for pairwise comparisons. All graphical representations were generated using Microsoft Excel or ggplot2 in R-Studio.

Objective 2: Statistical analyses were performed using R-Studio (version 2024.12.0) and Microsoft Excel. Prior to analysis, phenotypic data were checked for normality using the Shapiro-Wilk test. Frequency distributions were visualized by grouping data into predefined bin ranges to explore trait segregation patterns. Pearson correlation matrices were generated to evaluate relationships among phenotypic traits. For genetic mapping, the quality of the linkage map was evaluated by calculating both Pearson and Spearman correlation coefficient between the genetic and physical positions of loci. For gene expression analysis, differences between groups were analysed using an ANOVA followed by a Tukey's Honestly Significant Difference (HSD) test. Graphical representations were created using either Microsoft Excel or ggplot2 in R-Studio.

4. Results

Objective 1:

A total of eight dual-sgRNA CRISPR/Cas9 expression constructs were generated; three targeting *FaTFL1* and five targeting *FaFT1* (**Table 1**). Subsequently, a total of 81 and 11 transformed *Fragaria* × *ananassa* cvs. 'Calypso' and 'Malling Centenary' plants were recovered, respectively. PCR amplification of the kanamycin resistance gene cassette confirmed transformation in 73 out of 81 regenerated 'Calypso' plants and in all 11 regenerated 'Malling Centenary' plants, showing transformation efficiencies above 50% in both cultivars (**Table 1**). Among the 'Calypso' plants, those transformed with vector pCG34.1 produced the highest number of transformed lines (n = 25), followed by vector pCG32.1 (n = 22). In 'Malling Centenary', the highest number of transformed lines (n = 6) was obtained using vector pCG09.1. A greater number of 'Calypso' plants were regenerated and transformed compared to 'Malling Centenary'. Despite this, the results demonstrate that although the overall regeneration rate was lower in 'Malling Centenary', the regenerated plants exhibited a high transformation success rate.

Table 1. Transformation efficiency of regenerated shoots.

Variety	Gene	Vector	sgRNA pair	TE (%) *
Calypso	*FaFT1*	pCG12.1	34 & 48	60% (12/16)
Calypso	*FaFT1*	pCG13.1	42 & 32	62.5% (5/8)
Calypso	*FaFT1*	pCG32.1	32 & 55	100 % (22/22)
Calypso	*FaFT1*	pCG33.3	55 & 29	90 % (9/10)
Calypso	*FaFT1*	pCG34.1	29 & 67	100 % (25/25)
Malling Centenary	*FaTFL1*	pCG09.1	6 & 20	100 % (6/6)
Malling Centenary	*FaTFL1*	pCG10.1	19 & 47	100 % (2/2)
Malling Centenary	*FaTFL1*	pCG30.1	20 & 12	100 % (3/3)

*Transformation efficiency (TE %) = regenerated shoot samples / transformed shoot samples

Fragment analysis by CE enabled the detection of mutations at several target sites of both 'Malling Centenary' and 'Calypso transformed lines (**Figure 2**). Six 'Malling Centenary' lines (M1-M6) were evaluated; among these, only lines M1 and M2 transformed with the pCG09.1 vector exhibited multiple allelic mutations at *FaTFL1* target site #6 and line M6 transformed with the pCG30.1 vector showed a potential mutation at target site #12 or #20. A total of sixty-six 'Calypso' transformed lines were tested, of which forty-eight showed mutations at one or two of the *FaFT1* target sites. Within the six lines transformed with the pCG12.1 vector, mutations at target site #48

were detected in lines C1, C2, C3, and C6. In contrast, no edits were detected in the four lines (C7-C10) transformed with the pCG13 vector.

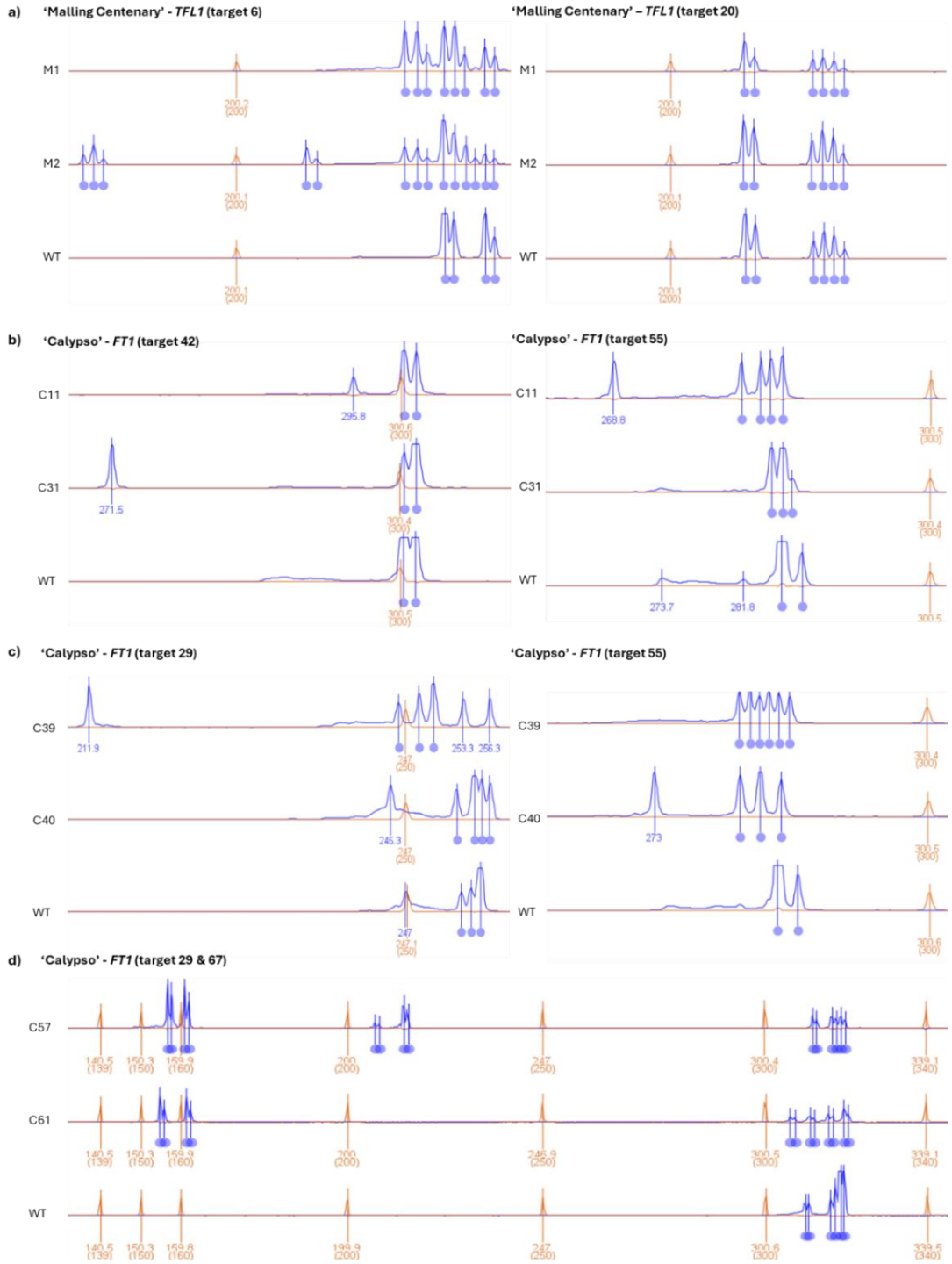

Figure 2. Detection of induced CRISPR/Cas9 mutations using fragment analysis by CE of target sites from representative mutant lines and wild type (WT). Electropherogram plots showing LIZ500 internal size standard peaks (orange) and 6-FAM labelled sample peaks (blue). **a)** *FaTFL1* target sites #6 and #20 in 'Malling Centenary' lines transformed with vector pCG09.1; **b)** *FaFT1* target sites #32 and #55 in 'Calypso' lines transformed with vector pCG32.1; **c)** *FaFT1*

target sites #29 and #55 in ‘Calypso’ lines transformed with vector pCG33.3; **d)** *FaFT1* target sites #29 and #67 in ‘Calypso’ lines transformed with vector pCG34.1.

From the 22 lines transformed with vector pCG32.1, eighteen showed indels, with the majority occurring at target site #55. Notably, lines C11 and C31 exhibited mutations at both target sites (#42 and #55) (**Figure 2b**). Similarly, 8 out of 9 lines transformed with vector pCG33.3 (C34-C41) displayed edits at one or both target sites, with lines C39 and C40 showing mutations on both target sites (**Figure 2c**). For vector pCG34.1, 18 of the 24 transformed lines had mutations at target site #29 and/or #67, with lines C57 and C61 showing multiple allelic mutations (**Figure 2d**). These results suggest that gRNAs targeting *FaTFL1* site #6 and *FaFT1* sites #29, #42, #46, #55, and #67 are functionally effective for the mutation of these genes.

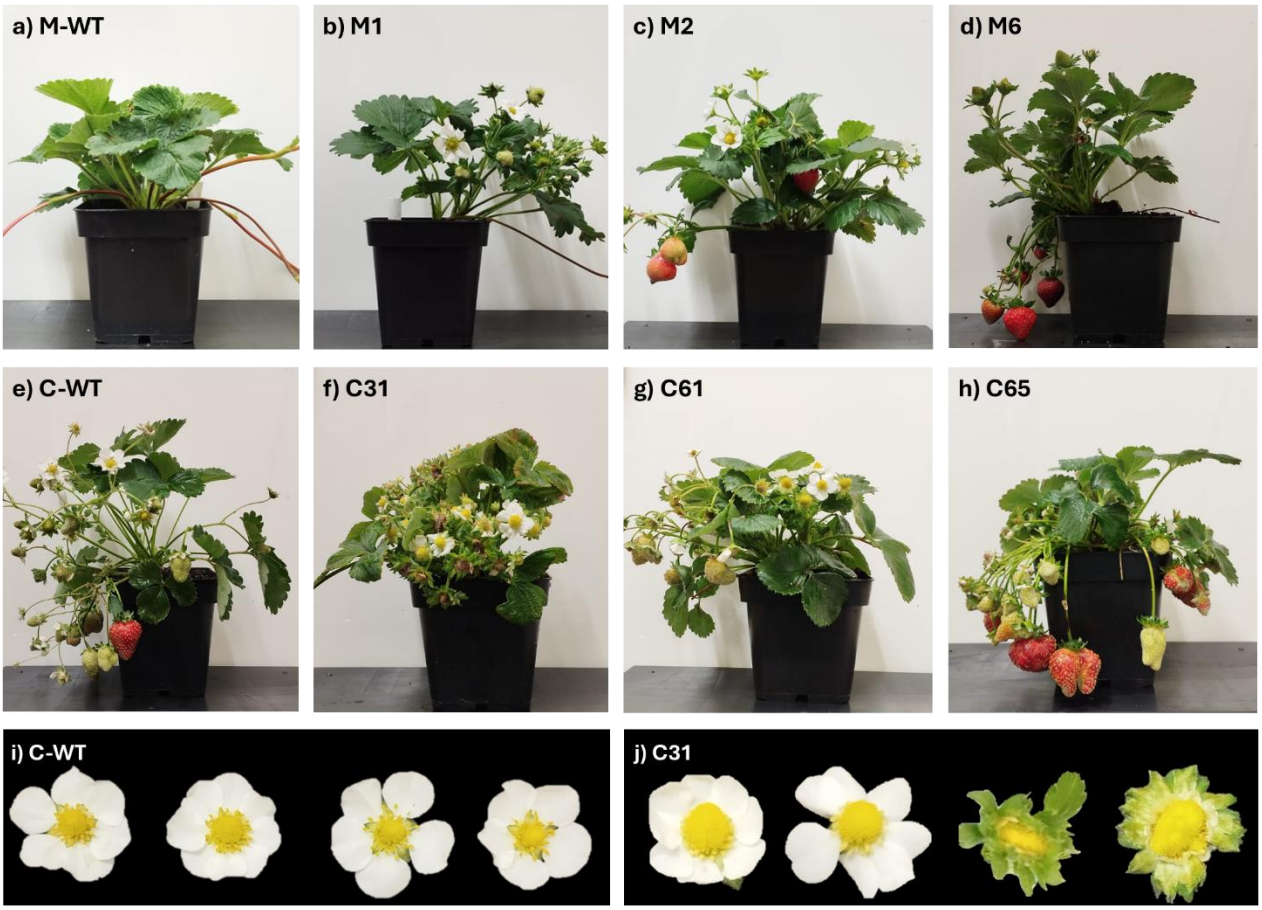

Figure 3. Phenotypic effects of mutation in *FaTFL1* and *FaFT1* mutant lines after five months under long days (LDs). **a)** Malling Centenary’ wild-type control (M-WT); **b-d)** *FaTFL1* mutant lines; **e)** ‘Calypso’ wild-type control (C-WT); **f-h)** *FaFT1* mutant lines; **i)** Open flowers of ‘Calypso’ wild-type control (C-WT); **j)** Examples of open flowers of ‘Calypso’ C31 mutant lines.

‘Malling Centenary’ *FaTFL1* mutant lines M1, M2, and M6, and ‘Calypso’ *FaFT1* mutant lines C3, C31, C61, and C65 were selected for phenotypic evaluation based on their editing profiles. Under

long day conditions, *FaTFL1* mutant lines flowered earlier than WT lines, which remained vegetative for more than three months (**Figure 3a-d**). Flowering time varied among the *FaTFL1* mutant lines, ranging from 39 days (M2), 49 days (M1), and 88 days (M6) compared to 97 days of the WT line (**Figure 4a**).

Significant differences in inflorescence number, compared to the WT were observed in lines M1 and M2, which produced an average of eight inflorescences per plant, compared to an average of two in the WT plants that flowered (n=11/19). In contrast, line M6 showed no significant difference in inflorescence production (**Figure 4b**). A similar trend was observed in total flower production: lines M1 and M2 produced an average of 31 flowers per plant, whereas WT and M6 lines produced an average of 16–19 flowers (**Figure 4c**).

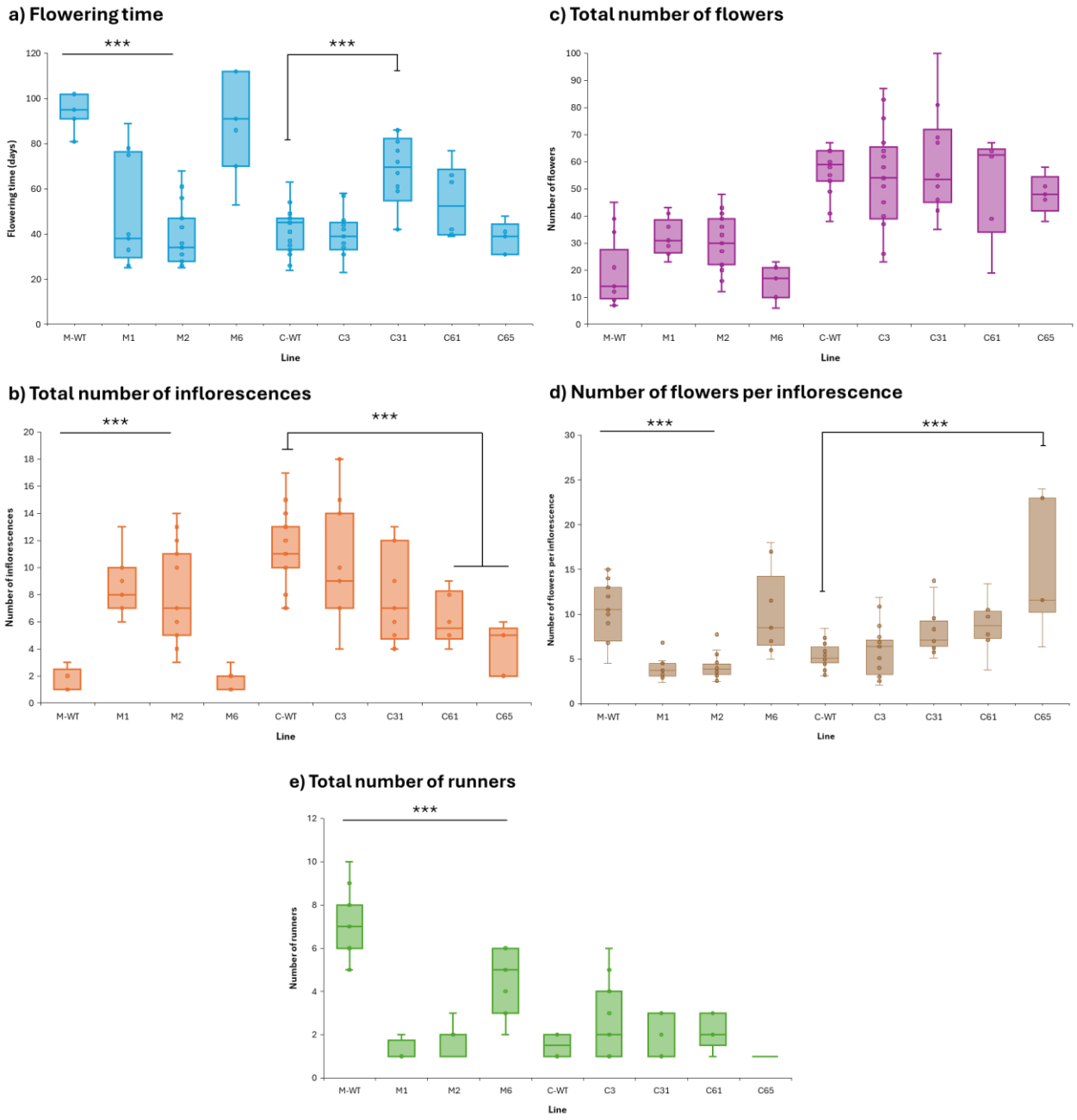

Figure 4. Phenotypic characterization of representative mutant and wild type (WT) lines grown under long days (LDs): a) Flowering time; **b)** Total number of inflorescences; **c)** Total number of flowers; **d)** Number of flowers per inflorescence (total number of flowers/total number of inflorescences; **e)** Total number of runners.

Despite the higher number of inflorescences and flowers produced in M1 and M2 compared to WT, these mutant lines exhibited altered inflorescence architecture, producing significantly fewer flowers per inflorescence. Specifically, M1 and M2 averaged 4 ± 1.3 flowers per inflorescence, compared to 11 ± 3.5 in WT and 10 ± 5.3 in M6 (**Figure 4d**). This suggests that mutation of the

FaTFL1 gene affects not only flowering quantity but also inflorescence development. Additionally, *FaTFL1* mutants showed reduced runner production compared to WT, which aligns with the increased flowering observed in these lines and indicates an effect in vegetative development (**Figure 4e**). Overall, M1 and M2 have similar phenotypes while M6 shows a weak phenotype closely resembling the WT.

'Calypso' *FaFT1* mutant lines C31 and C61 exhibited delayed flowering, with average flowering times of 67 and 55 days, respectively, compared to 41 days in the WT (**Figure 4a**). Lines C3 and C65, however, showed no significant difference, both averaging 39 days to flowering. Notable differences in inflorescence architecture and floral morphology were observed in the *FaFT1* mutant lines compared to the WT (**Figures 3e–h**). Lines C31, C61, and C65 displayed compact growth and signs of fasciation, characterized by underdeveloped, fused, and compacted inflorescences and flowers. These abnormalities were particularly pronounced in lines C31 and C65, which exhibited flattened and elongated floral structures (**Figures 3i–j**).

Despite these architectural changes, there was no significant difference in the total number of flowers produced per plant compared to the WT, with all lines averaging between 54 and 58 flowers (**Figure 4c**). Similarly, most *FaFT1* mutant lines did not differ significantly from the WT in the number of flowers per inflorescence: C3 averaged 6 ± 2.9, C31 averaged 8 ± 3.0, and C61 averaged 9 ± 3.3, compared to 5 ± 1.5 in the WT. The exception was line C65, which produced significantly more flowers per inflorescence, averaging 15 ± 8 (**Figure 4d**). No significant differences were observed in runner production between the *FaFT1* mutants and the WT, with all lines averaging two runners per plant (**Figure 4e**).

Objective 2:

Significant phenotypic variations were observed between the parental lines (ES12 and ICE12) for the four evaluated traits (Runner count, leaf count during short day (SD) treatments, leaf count to flower and flowering time) (**Figure 1**). During the autumn treatment, runner count varied significantly between parents, as ES12 produced an average of 11 while ICE12 produced 2, confirming that ES12 continues to produce runners under SD conditions (**Figure 1a**). However, both parents produced an average of only 2 runners during the winter treatment, indicating that runner formation is equally suppressed at low temperatures (≥6°C). Leaf count during SD treatments varied between parents, with ES12 producing more leaves (autumn: 9; winter: 10) than ICE12 (autumn:8; winter: 5) (**Figure 1b**). The same pattern was observed for leaf count to flower, with ES12 producing more leaves (autumn: 14; winter: 12) than ICE12 (autumn:8; winter: 8) (**Figure 1c**). Flowering time also varied significantly between genotypes (**Figure 1d**). ES12

flowered later after the autumn treatment ($\bar{x}$ = 43 days) compared to ICE12 ($\bar{x}$ =26 days). However, after the winter treatment ES12 flowered earlier ($\bar{x}$ =12 days) than ICE12 ($\bar{x}$ =40 days). These results demonstrate that ICE12 and ES12 exhibit genotype-specific responses to seasonal SD treatments, influencing both vegetative growth and the timing of floral transition.

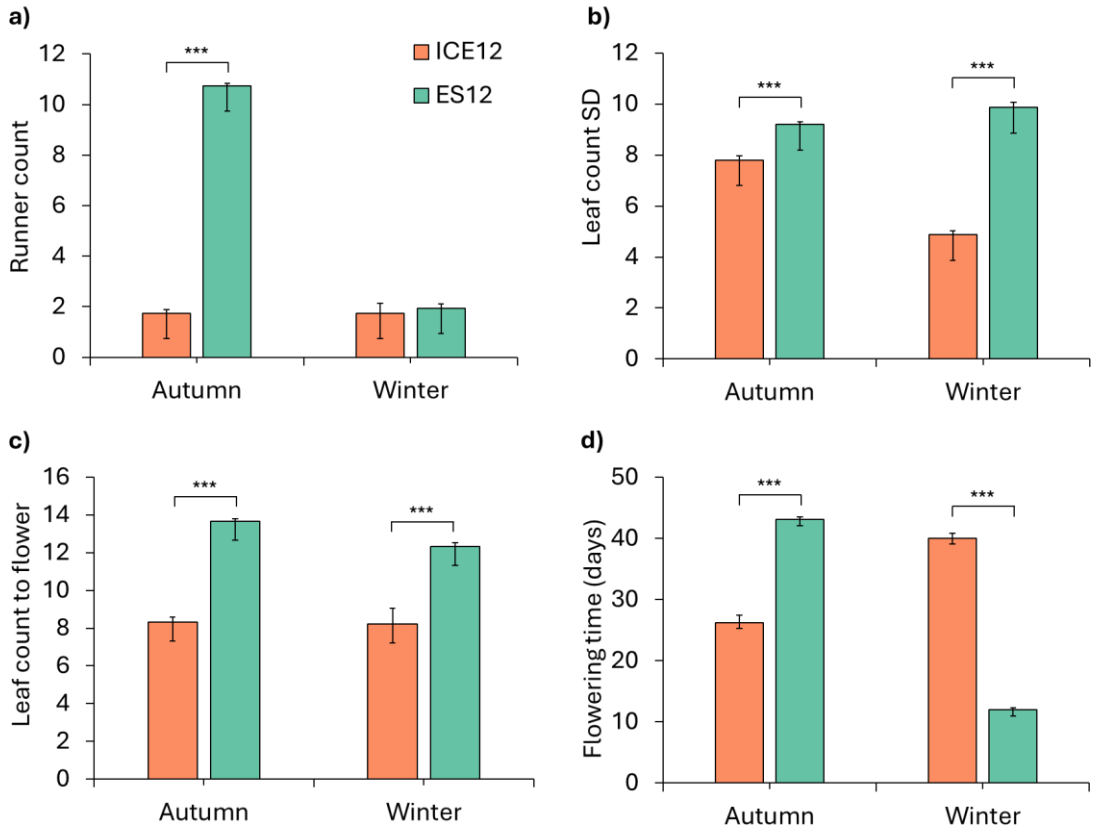

Figure 1. Phenotypic variation between parental lines (ICE12, ES12) grown under different SD treatments. a) Runner count; **b)** Leaf count during SD treatments; **c)** Leaf count to flower; **d)** Flowering time. Autumn treatment: 6 weeks at 11°C, 12-hour photoperiod; Winter treatment: 12 weeks at 6 °C, 12-hour photoperiod. Data are presented as mean ± standard error, n = 15-30. Asterisks indicate statistically significant differences between parental lines within each treatment (****P < 0.001*, Student's t-test).

Segregation of all four phenotypic traits was observed in the F_2 mapping population (**Figure 2**). During E1, individuals produced between 1 and 12 runners, with the highest proportion (36.9%) falling within the 2–3 runner range (**Figure 2a**). Flowering time ranged from 3 to over 75 days, with the highest proportion of individuals (27.9%) flowering between 30 and 34 days (**Figure 2b**).

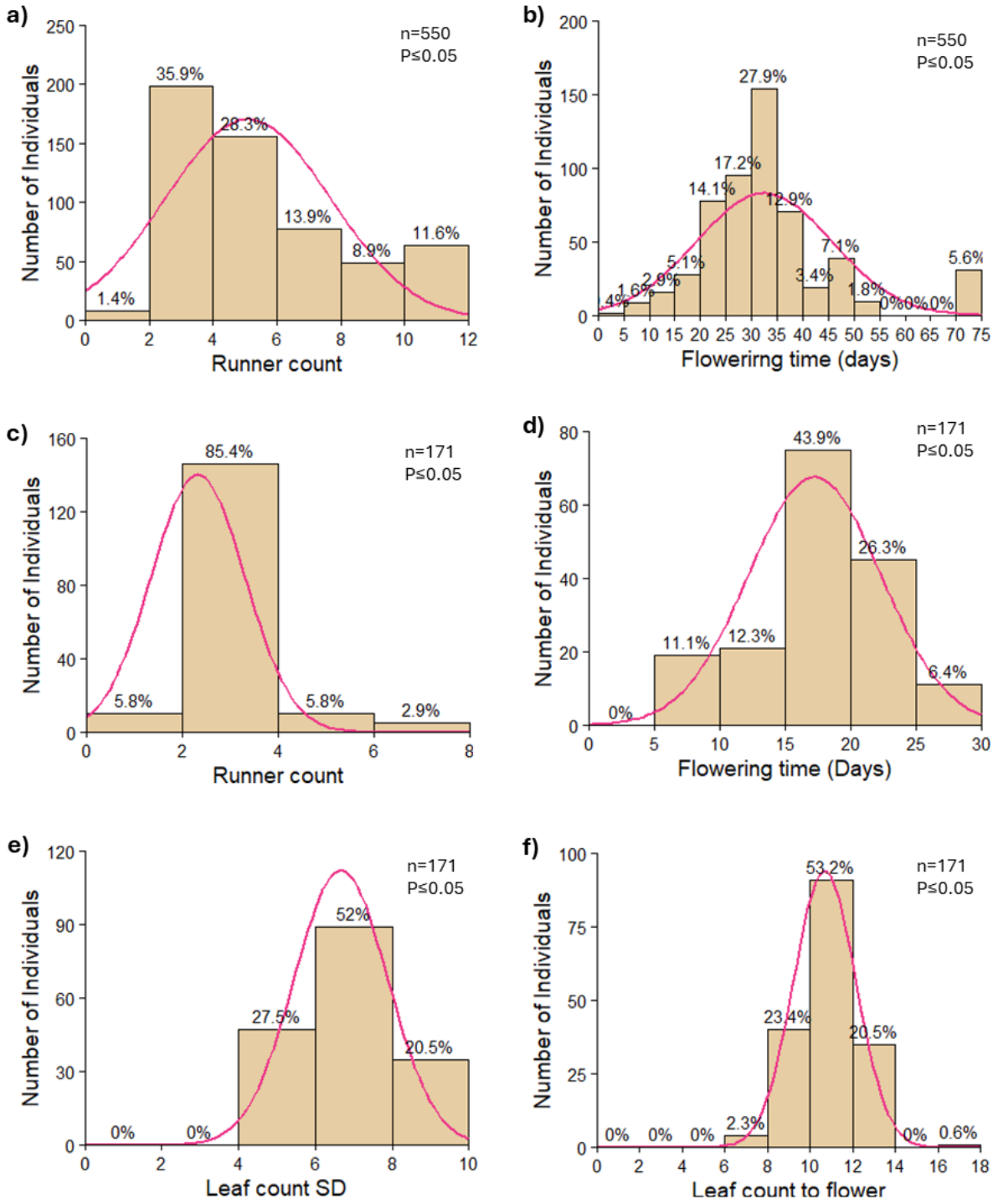

Figure 2. Phenotypic variation in the ES12xICE12 F_2 population in Experiment 1 (E1) and Experiment 2 (E2). Frequency distribution of **a)** Runner count-E1; **b)** Flowering time-E1; **c)** Runner count-E2; **d)** Flowering time-E2; **e)** Leaf count during SD treatments-E2; **f)** Leaf count to flower-E2. Histogram bins include the lower bound and exclude the upper bound. The value at the top of each bar represents the percentage of individuals within that range of trait value. The magenta line indicates the trait distribution curve. The number of individuals analysed is shown in the top-right corner of each panel, and the p-value from the Shapiro-Wilk normality test is displayed below (*p ≤0.05* indicates a non-normal distribution).

In E2, which included a shorter autumn treatment, slight shifts in trait segregation were observed. Runner count ranged from 1 to 8 runners, with most individuals (85.4%) falling in the 2-3 runner range (**Figure 2c**). Flowering time occurred between 5 to 30 days, with the highest proportion of individuals (43.9%) flowering within the 15–19-day range (**Figure 2d**). Leaf number during SD treatments varied from 4 to 10, with the highest proportion of individuals (52%) producing 6-7 leaves (**Figure 2e**). The total number of leaves to flower ranged from 8 to 18, with the highest proportion of individuals (53.2%) producing 10-11 leaves prior to flowering (**Figure 2f**). All the traits showed a significantly non-normal distribution ($p < 0.001$) and a moderately high coefficient of variation (14-51%).

Pearson correlation coefficients were evaluated to determine the correlation between traits (**Figure 3**). No significant correlation was found between runner production during autumn and flowering time in E1 (r=0.09) (**Figure 3a**). However, in E2 a significantly negative correlation (r=-0.6) was observed between runner production during autumn and flowering time, suggesting that individuals that produce more runners during autumn tend to flower earlier after a long winter treatment (**Figure 3b**). Contrastingly, a significantly positive correlation was seen between runner production and leaf count during SD treatments (r=0.67) and during LD treatment prior to flowering (r=0.43), indicating that individuals that continue to produce runners also tend to produce more leaves during both treatments. In general, a high phenotypic variation and dispersion was seen for all the traits indicating complex segregation patterns potentially involving both major-effect QTLs and polygenic background variation. Together these results provide a foundation for subsequent QTL analysis of the continuous runnering trait.

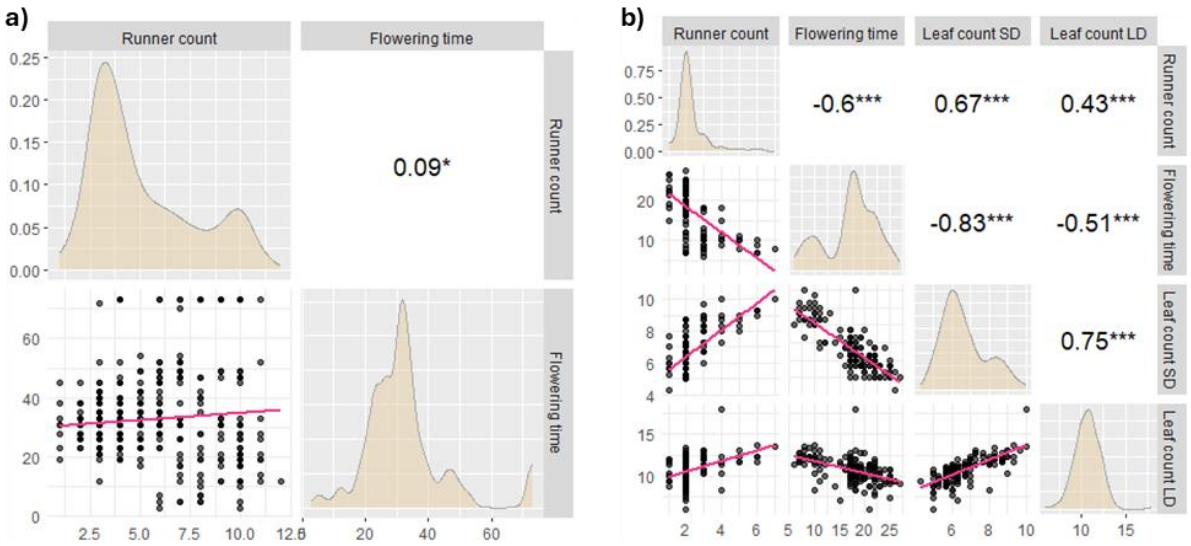

Figure 3. Correlation matrix of phenotypic traits in Experiment 1 (E1) and Experiment 2 (E2). **a)** Correlation between runner count and flowering time in E1; **b)** Correction between runner count,

flowering time, leaf count during SD treatments and leaf count to flowering (LD) in E2. Asterisks indicate different levels of significance (***p<0.0001, **p<0.01 or *p<0.05).

To identify genomic regions associated with continuous runnering, a genetic linkage map was constructed using GBS data from 90 individuals from the F_2 mapping population. To capture the genetic variation of the continuous runnering trait, the individuals selected consisted of 24.44% continuous runnering plants and 75.56% of plants with low number of runners. Initial variant calling resulted in 163858 loci based on the *F. vesca* 'Hawaii-4' reference genome v4.0. A total of 1258 loci were selected for genetic mapping based on their segregation pattern. Of these, 865 markers were successfully mapped to seven linkage groups corresponding to the seven chromosomes of the *F. vesca* genome.

The resulting linkage map spanned a total genetic distance of 398.21 cM, with each individual linkage group ranging from 26.22 to 82.92 cM in length. The average inter-marker genetic distance ranges between 0.3 and 0.7 cM, indicating a high marker density. The physical coverage of the map was a total of 210.67 Mb, representing approximately 87.25% of the *F. vesca* genome which is estimated at 240 Mb (Shulaev et al., 2011). A moderate to high correlation between the genetic and physical position of markers was observed, indicating that the marker order on the linkage map largely reflects their true genomic locations and distribution. A detailed summary of marker distribution, total genetic length, average inter-marker distance, and correlation for each linkage group is provided in **Table 2**.

Table 2. Characteristics of the ES12xICE12 F_2 genetic linkage map.

Linkage group	Genetic distance (cM)	Physical distance (Mb)	Mapped markers	Avg. marker distance (cM)	Correlation* (Pearson/Spearman)
Fvb1	48.36	19.41	161	0.3	0.874 / 0.996
Fvb2	45.73	29.12	70	0.7	0.782 / 0.987
Fvb3	70.84	38.10	150	0.5	0.933 / 0.996
Fvb4	51.71	33.80	128	0.4	0.664 / 0.988
Fvb5	72.53	29.10	114	0.6	0.879 / 0.994
Fvb6	82.82	39.78	175	0.5	0.939 / 0.998
Fvb7	26.22	21.36	67	0.4	0.899 / 0.996
Total	398.21	210.67	865	-	-

*Pearson correlation coefficient /Spearman rank correlation coefficient (values close to 1 indicate high correlation)

A QTL scan was performed using phenotypic data for all four traits from E1 and E2 (**Figure 4a**). A significant QTL was identified on chromosome Fvb4 and Fvb5 for runner count in E1. However, no QTLs were detected for flowering time in this experiment. Interestingly, a consistent QTL was identified on chromosome Fvb5 for runner count in E1 and E2, and for flowering time and leaf count during SD treatments in E2. No significant QTLs were found for leaf count to flower in E2.

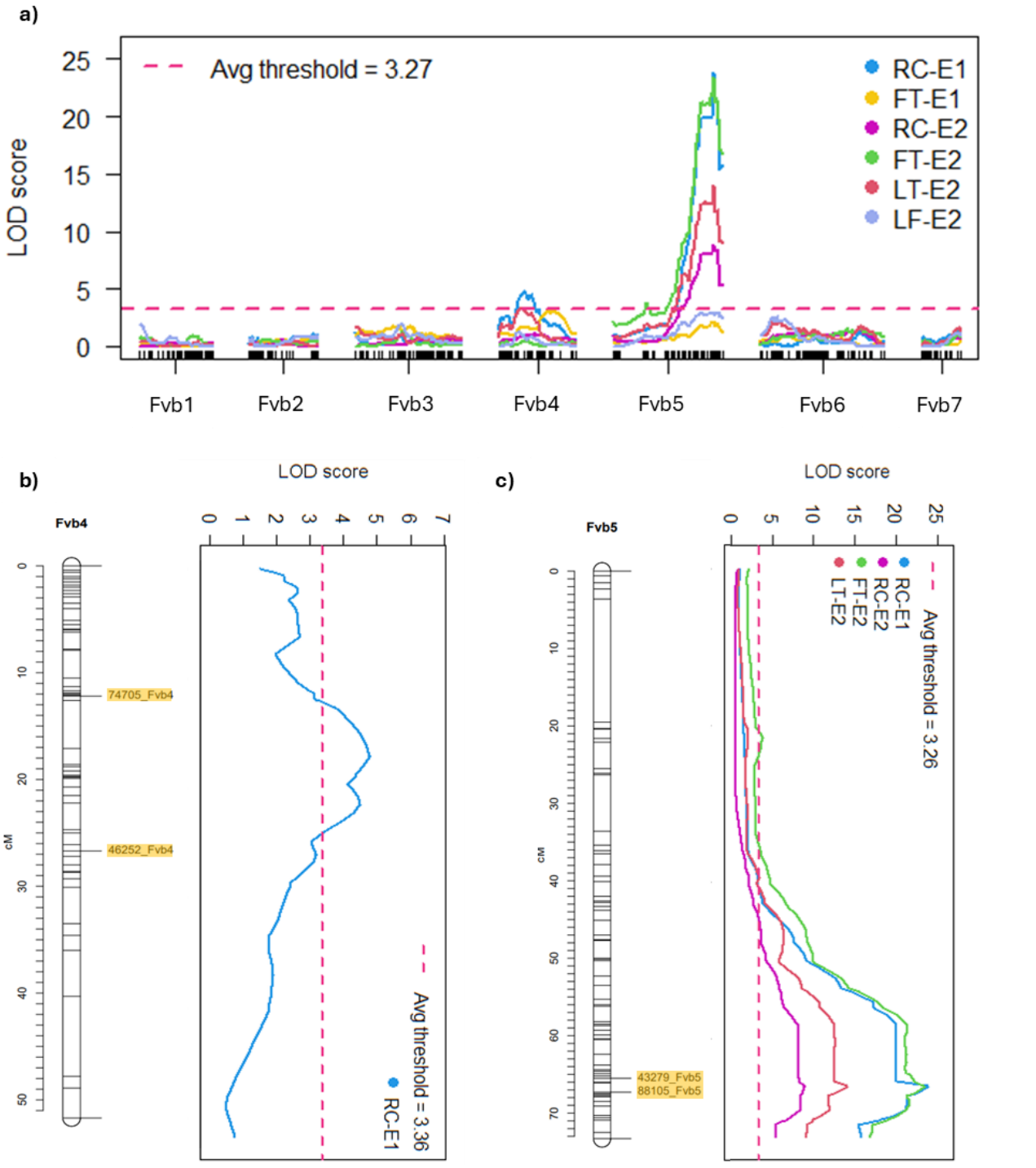

Figure 4. QTL scan for continuous runnering associated traits. a) QTL scan of runner count (RC), flowering time (FT), leaf count during SD treatments (LT) and leaf count to flower (LF) from Experiment 1 (E1) and Experiment 2 (E2); **b)** Minor QTL identified on chromosome Fvb4 and position on the genetic map; **c)** Major QTL identified on chromosome Fvb5 and position on the genetic map. Each trait evaluated is represented by a distinct colour, as shown in the top-right legend. The dashed magenta line indicates the average genome-wide LOD significance threshold (α = 0.05), calculated from 1,000 permutations performed separately for each trait. QTL flanking loci positions are highlighted in yellow on the genetic maps.

The QTL detected on chromosome Fvb4 for runner count from E1(RC-E1), spans a 2.7 Mb region flanked by locus 74705 and 46252 (**Figure 4b**). The peak LOD score averaged at 4.35, slightly exceeding the whole genome significance threshold of 3.36. This QTL explained between 16 and 22% of the phenotypic variance in runner count, with a high additive effect and a low dominance deviation, suggesting a minor to moderate genetic influence on the trait and an additive mode of inheritance.

The QTL detected on chromosome Fvb5 for runner count, flowering time and leaf count during SD treatments, spanned a 2.4 Mb region flanked by locus 43279 and 88105 (**Figure 4c**). The average peak LOD scores between the traits ranged from 8.82 to 23.51, significantly above the average whole genome significance threshold of 3.27. This QTL explained between 64-71% of the observed phenotypic variance for runner count from E1 (RC-E1), 34-36% for runner count from E2 (RC-E2), 68-70% for flowering time from E2 (FT-E2) and 45-51% for leaf count during SD treatments from E2 (LT-E2), indicating a major genetic influence on these traits. The QTL for runner counts and leaf count during SD treatments, exhibited a high additive effect and a low dominance deviation, suggesting a predominantly additive mode of inheritance. In contrast, the QTL for flowering time, showed a low additive effect and hight dominance deviation, suggesting a different inheritance pattern. A summary of the QTL analysis is shown in **Table 3**.

Table 3. Analysis of significant QTLs on chromosome Fvb4 and Fvb5.

Trait	Linkage group	Flanking markers	Region Size (Mb)	LOD Peak (min-max)	% Variance Explained	Avg. Additive	Avg. Dominance
RC-E1	4	74705 – 46252	2.7	3.42 – 4.77	16 – 22%	1.58	–0.57
RC-E1	5	43279 – 88105	2.4	19.97 – 21.35	64 – 71%	2.79	–2.50
RC-E2	5	43279 – 88105	2.4	8.17 – 8.32	34 – 37%	0.62	–0.48
FT-E2	5	43279 – 88105	2.4	22.06 – 23.51	68 – 70%	–6.4	1.85
LT-E2	5	43279 – 88105	2.4	11.72 – 13.96	45 – 51%	1.05	–1.06

To validate the major QTL found on chromosome Fvb5, CAPS markers for the loci 43279 and 88105 flanking the QTL region were developed for genotyping. The parental lines, the F_1 hybrid, 251 individuals from the F_2 mapping population and 120 individuals from the F_2 validation population were genotyped using these markers and scores of the allelic state of the two markers were compared with phenotypic data. The continuous runnering parent ES12 carried a homozygous genotype, labelled A, the parent with normal cessation of runnering ICE12 showed a

homozygous genotype, labelled B and the F_1 hybrid exhibit a heterozygous H genotype for both markers (43279:88105).

Phenotypic observations of runner count were consistent with the parental genotypes across the mapping population and the validation population. Individuals with genotype A generally produced more runners than those with genotype B or H (**Figure 5a-c**). A lower average runner count was observed in A genotypes in E2 than in E1 or E3, which included a longer autumn treatment, or only had an autumn treatment, respectively. Individuals from both populations, also showed consistent genotypic/phenotypic association patterns for flowering time, with variation across SD treatments that reflected the differences observed in the parental lines. Individuals with genotype A flowered earlier than the other genotypes in E1 and E2 with winter treatments, but later in E3 that only included an autumn treatment, as observed previously in ES12 (**Figure 5d-f**). Additionally, phenotypic observations of leaf production during SD treatments (LT) and prior to flowering (LF) in E2 also aligned with the genotypic and phenotypic pattern observed in the parents. Individuals with genotype A, produced in general more leaves during both treatments than the other genotypes (**Figure 5g-h**).

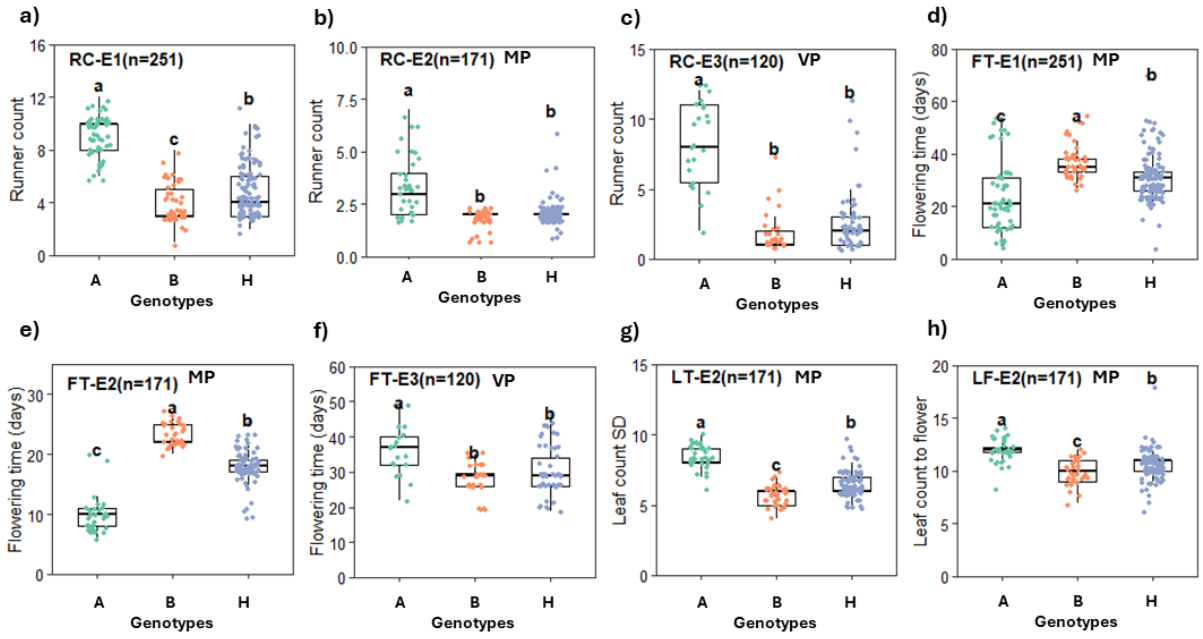

Figure 5. Effect of QTL on continuous runnering and associated phenotypic traits. Evaluation was done in the F_2 mapping (MP) and validation population (VP) under different experimental setups (E1-E3). The plots show the QTL effect on **a-c)** runner count (RC); **d-f)** flowering time (FT); **g)** leaf count during SD treatments (LT); **h)** leaf count to flower (LF). The population type, phenotypic experiment setup and number of individuals evaluated are shown in the upper left corner of the plots. Letters above each box indicate significance groups based on Tukey's HDS test following ANOVA ($p<0.05$).

Among the individuals genotyped, three recombinants for the continuous runnering A genotype were identified in the mapping population (#17, 101,161) and two in the validation population (#18, #43) (**Figure 6**). These individuals displayed either an A:H or H:A genotype recombination profile for the CAPS flanking markers (43279:88105). Recombinants with an A:H profile did not show continuous runnering, while recombinants with an H:A profile had a continuous runnering phenotype, indicating that the candidate genes conferring this trait are likely located in the lower end of the locus.

					MP*			VP*	
Marker	Position (Mb)	ES12	ICE12	F1	101	161	17	43	18
43279	23.74	**A**	**B**	**H**	**A**	**A**	**H**	**H**	**A**
29996	23.77	A	B	H	A	H	H	H	A
71693	23.7	A	B	H	A	H	H	H	A
19137	23.78	**A**	**B**	**H**	**A**	**H**	**H**	**H**	**A**
107061	23.80	A	B	H	A	H	H	H	A
40240	23.86	A	B	H	A	H	H	H	A
99840	24.17	**A**	**B**	**H**	**A**	**H**	**H**	**H**	**A**
35931	24.21	A	B	H	A	H	H	H	A
104105	24.28	A	B	H	A	H	H	H	A
101499	24.28	**A**	**B**	**H**	**A**	**H**	**H**	**H**	**A**
20307	24.34	A	B	H	A	H	A	A	H
89672	24.57	**A**	**B**	**H**	**A**	**H**	**A**	**A**	**H**
52904	24.57	A	B	H	A	H	A	A	H
10458	24.60	A	B	H	A	H	A	A	H
6976	24.63	A	B	H	A	H	A	A	H
26819	24.82	A	B	H	A	H	A	A	H
1267	24.91	**A**	**B**	**H**	**A**	**H**	**A**	**A**	**H**
104611	24.96	A	B	H	A	H	A	A	H
I_5g35400	25.93	**A**	**B**	**H**	**A**	**H**	**A**	**A**	**H**
Runnering phenotype*		**1**	**0**	**0**	**1**	**0**	**1**	**1**	**0**
88105	26.19	**A**	**B**	**H**	**H**	**H**	**A**	**A**	**H**

Narrow QTL region

*MP: F_2 mapping population (MP); VP: F_2 validation population; 1=continuous runnering; 0=low runnering

Figure 6. Fine mapping of major QTL associated with continuous runnering on chromosome Fvb5. Genotype of parents (ES12, ICE12), F_1 hybrid, and recombinant individuals from the F_2 mapping population (MP) and validation population (VP) are shown for seven CAPS markers (green) and an indel marker (blue) for gene *FvH_5g35400* identified within the QTL region. Genotype A: homozygous for the ES12 allele; Genotype B: homozygous for the ICE12 allele; Genotype H: heterozygous. Genotypes shown in bold are confirmed and genotypes in light

grey are imputed. Phenotypes for all individuals are indicated in red (1=continuous runnering; 0=low runnering). Dash lines indicate recombination breakpoints.

To further narrow down the QTL region,186 out of 265 individuals analysed previously were genotyped with two additional markers, 19137 and 89672, located within the interval. The five recombinant individuals were also genotyped with three more makers (99840, 101499 and 1267) to better define recombination breakpoints. This analysis identified a further recombination point between markers 101499 and 88105 in individuals 17, 18 and 43. Additionally, all 265 individuals were genotyped with a marker targeting a 120 bp indel found in the gene *FvH4_5g35400*, positioned at 2.59 Mb and located between markers 1267 and 88105 of the QTL intervals. The indel was identified from unpublished NGS data from the parental lines (data not shown).

These markers further refined the recombination breakpoint and demonstrated that all recombinant individuals with the continuous runnering phenotype were homozygous (A) from marker 101499, while their genotype at flanking marker 88105 varied (A or H). These results narrow the candidate region to a 1.91 Mb interval between markers 101499 and 88105, suggesting that the causal gene(s) for the continuous runnering trait likely reside within this segment, as recombination after the indel marker (I_5g35400) did not disrupt the phenotype.

A total of 1622 and 765 genes were identified within the QTL regions on chromosome Fvb4 and Fvb5 respectively. In the QTL on linkage group four, two *MADS*-Box genes (*FvH4_4g27110* and *FvH4_4g27440*) and a *TEOSINTE BRANCHED 1*, *CYCLOIDEA*, and *PROLIFERATING CELL FACTORS 7* (*TCP7*) transcription factor (*FvH4_4g31520*) were selected as strong candidates due to reported roles of homologous genes in regulating dormancy, flowering time and growth in other species (Hartmann et al., 2000; Wu et al., 2017; Kieffer et al., 2011; Wei et al., 2016). In the QTL on linkage group five, five potential genes (*FvH4_5g34080, FvH4_5g34500, FvH4_5g34860, FvH4_5g35400, FvH4_5g3540*1) were selected as major targets. These include *MADS*-box genes and other developmental genes previously reported to play roles in the regulation of dormancy, vernalization, flowering time, and the transition from vegetative to reproductive phase (Hartmann et al., 2000; Wu et al., 2017; Dong et al., 2023; Chen et al., 2024; Kim et al., 2022; Sung and Amasino, 2004; Greb et al., 2007; Michaels et al., 2003). Within these, *FvH4_5g35400* which is an *SVP/JOINTLESS-like* gene was identified as the most promising candidate due to its position within the QTL region on chromosome Fvb5 and the indel previously identified.

Table 4. Summary of candidate genes identified for significant continuous runnering QTL on chromosome Fvb4 and Fvb5.

ID_*F.vesca* (Position)	LG	Arabidopsis (Homolog)	Name (annotation)	Gene function	Associated role (ref*)
FvH4_4g27110 (28.23 Mb)	Fvb4	AT2G22540.3	*SVP-like (SHORT VEGETATIVE PHASE)*	DNA binding	Regulation of dormancy and flowering time (1,2)
FvH4_4g27440 (28.44 Mb)	Fvb4	AT2G22540.3	*SVP-like/AGL24 (SHORT VEGETATIVE PHASE/ AGAMOUS-like 24)*	DNA binding	Regulation of dormancy and flowering time (1,2)
FvH4_4g31520 (30.61 Mb)	Fvb4	AT3G47620.1	*TCP7 (TEOSINTE BRANCHED 1, CYCLOIDEA, and PROLIFERATING CELL FACTORS)*	DNA binding	Cell proliferation and internode elongation (3)/Growth and development (4)
FvH4_5g34080 (2.47 Mb)	Fvb5	AT3G57230.4	*AGL16 (AGAMOUS-like 16)*	DNA binding	Regulation of flowering time (5)/AXB outgrowth (6)
FvH4_5g34500 (2.51 Mb)	Fvb5	AT4G24470.2	*ZIM-like 1/GATA25 (GATA transcription factor 25)*	DNA binding	Regulation of flowering time (7)
FvH4_5g34860 (2.55 Mb)	Fvb5	AT4G30200.3	*VEN5/VIN3-like (VERNALIZATION 5/VERNALIZATION INSENSITIVE 3)*	DNA binding	Regulation of vernalization and flowering time (8,9)
FvH4_5g35400 (2.59 Mb)	Fvb5	AT2G22540.3	*SVP1/JOINTLESS-like (SHORT VEGETATIVE PHASE)*	DNA binding	Regulation of dormancy and flowering time (1,2)
FvH4_5g35401 (2.59 Mb)	Fvb5	AT2G22540.3	*AGL24 (AGAMOUS-like 24)*	DNA binding	Regulation of floral organ identity (10)

*Ref: (1) Hartmann et al., (2000); (2) Wu et al., (2017); (3) Kieffer et al., (2011); (4) Wei et al., (2016); (5) Dong et al., (2023); (6) Chen et al., (2024); (7) Kim et al., (2022); (8) Sung and Amasino, (2004); (9) Greb et al., (2007); (10) Michaels et al., (2003).

Individuals from the validation population with significant phenotypic differences were used to analyse the expression levels of four of the candidate genes (*FvH4_4g27110*, *FvH4_4g27440*, *FvH4_5g35400*, *FvH4_5g35401*). Gene expression was first analysed under LD conditions (summer treatment) before the start of E3, and subsequently under SD conditions (autumn treatment) during E3. The results showed noticeable variations in gene expression levels between genotypes and within treatments for most of the genes (**Figure 7**).

The expression levels of *FvH4_4g27110* did not differ significantly between genotypes under both treatments (**Figure 7a**). The expression of *FvH4_4g27440* did not differ significantly between genotypes during the summer treatment, however, there was a small variation in expression during autumn treatment, with genotype A showing a significantly lower expression than B and H (**Figure 7b**). The expression of *FvH4_5g35400* differed significantly between genotypes during both summer and autumn conditions, as genotype A showed almost no expression while genotype B showed the highest followed by H (**Figure 7c**). The expression in B and H genotype also increased from summer to autumn treatments. The expression of *FvH4_5g35401* was also significantly lower in genotype A compared to the other two genotypes in both treatments, although it maintained a similar expression level between the treatments (**Figure 7d**).

In summary, the results show that *FvH4_5g35400* is the only gene that not expressed during both treatments in A continuous runnering individuals, and its expression level markedly increased in B and intermediate H genotypes in the autumn treatment. Furthermore, a similar expression pattern was seen for genes *FvH4_4g27440* in A genotypes specifically in the autumn treatment and in *FvH4_5g35401* in both treatments. However, among all the genes, *FvH4_5g35400* showed the highest expression levels in genotypes B and H.

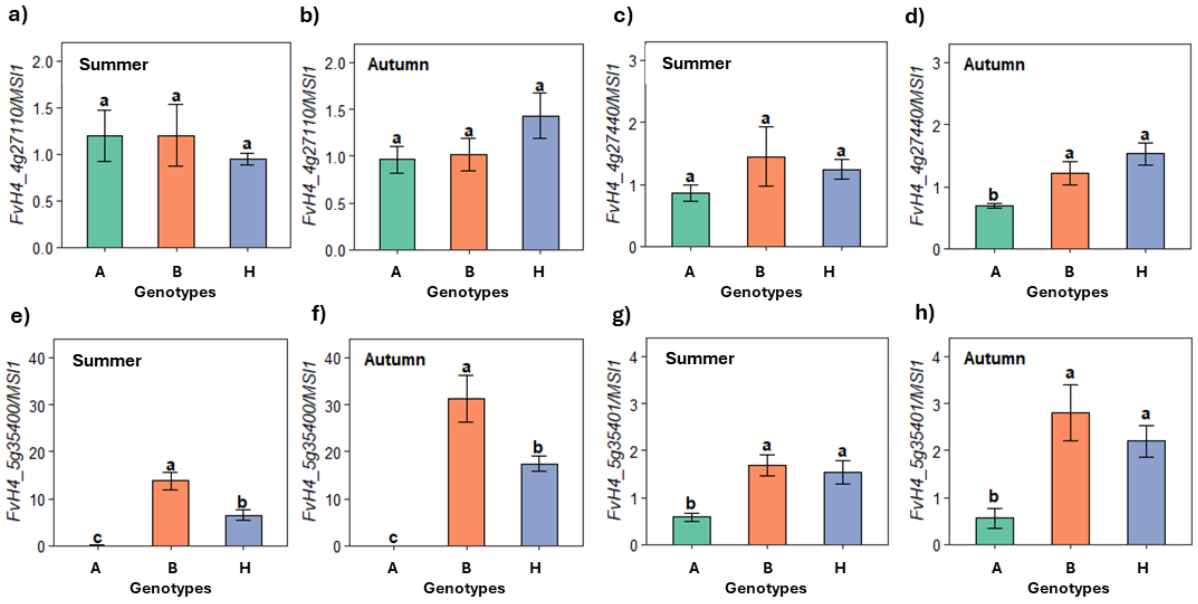

Figure 7. Gene expression analysis of candidate genes in genotypes A, B, and H from the F_2 validation population under summer and autumn treatments. Plots show the relative expression levels (ΔΔCt) of candidate genes normalized to the control gene *FvMSI1*, for the following candidate genes: **a-b)** *FvH4_4g27110* (*SVP-like*); **c-d)** *FvH4_4g27440* (*SVP-like/AGL24*); **e-f)** *FvH4_5g35400* (*SVP/JOINTLESS-like*); **g-h)** *FvH4_5g35401* (*AGL24*). Genotype A= homozygous for the ES12 A alleles, genotype B= homozygous for ICE12 B alleles, genotype

H=heterozygous for A and B alleles). Letters above each bar indicate significance groups based on Tukey's HDS test following ANOVA ($p<0.05$).

Objective 3:

A total of six dual-sgRNA CRISPR/Cas9 expression constructs were developed: two targeting *FvH4_ 5g35400*, two targeting *FvH4_ 5g35401*, and two targeting both genes (**Table 2**). A total of 49 plants were regenerated and PCR amplification of the kanamycin resistance gene cassette confirmed successful transformation of 46 of these. Transformation efficiencies exceeded 50% for all constructs, except for pCG51.1, from which no plants were regenerated. The lowest number of transformed lines was obtained with vector pCG51.1 and pCG52.1 for *FvH4_ 5g35401*, while nine transformed lines were obtained with each of the other vectors targeting *FvH4_ 5g35400* or both genes.

Table 2. Transformation efficiency of regenerated shoots.

Gene (s)	Vector	gRNA pair	TE (%) *
FvH4_ 5g35400	pCG47.1	42 & 49	90% (9/10)
FvH4_ 5g35400	pCG48.1	15 & 27	69% (9/13)
FvH4_ 5g35401	pCG51.1	39 & 68	0% (0/0)
FvH4_ 5g35401	pCG52.1	49 & 50	67% (4/6)
FvH4_ 5g35400 /FvH4_ 5g35401	pCG53.1	42 & 39	100% (9/9)
FvH4_ 5g35400 /FvH4_ 5g35401	pCG55.1	15 & 44	100% (9/9)

*Transformation efficiency (TE %) = regenerated shoot samples / transformed shoot samples

A total of 43 lines were evaluated through fragment analysis (**Figure 1**). Mutations in *FvH4_5g35400* were observed in multiple transformation groups. Eight of the lines transformed with vector pCG47.1 (M1, M2, M5, M6, M7, M8, M9, M10) carried mutations only at target site 49, while three of the lines transformed with pCG48.1 (M11, M12, M16) showed mutations only at site 27. Two of the lines transformed with pCG53.1(M29, M34) showed mutations at target site 42, while six of the lines (M36, M37, M38, M39, M40, M42) transformed with pCG55.1 showed mutations only at target site 15. Line M12 transformed with pCG48.1 was the only line to carry mutation in both target sites 15 and 27. For *FvH4_5g35401*, four lines (M24, M25, M26, M27) transformed with vector pCG52.1 exhibited mutations only at target site 50.

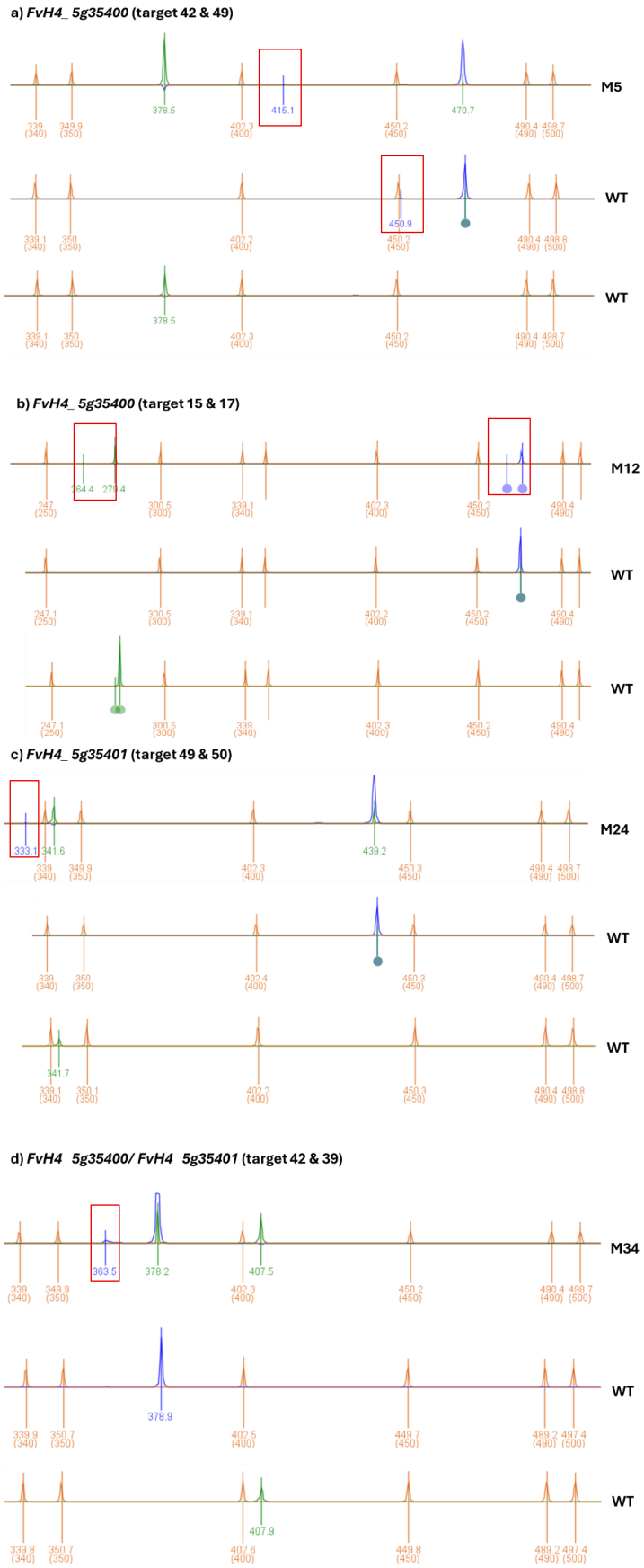

Figure 1. Detection of induced CRISPR/Cas9 mutations using fragment analysis by capillary electrophoresis (CE) of target sites from representative mutant lines and wild type (WT).

Electropherogram plots showing LIZ500 internal size standard peaks (orange), 6-FAM labelled sample peaks (blue) for the first target and HEX labelled sample peaks (green) for the second target. **a)** *FvH4_5g35400* target sites 42 and 49; **b)** *FvH4_5g35400* target sites 15 and 17; **c)** *FvH4_5g35401* target sites 49 and 50; **d)** *FvH4_5g35400/ FvH4_5g35401* target sites 42/39. The additional peaks shown in a red box were taken to indicate a potential mutation.

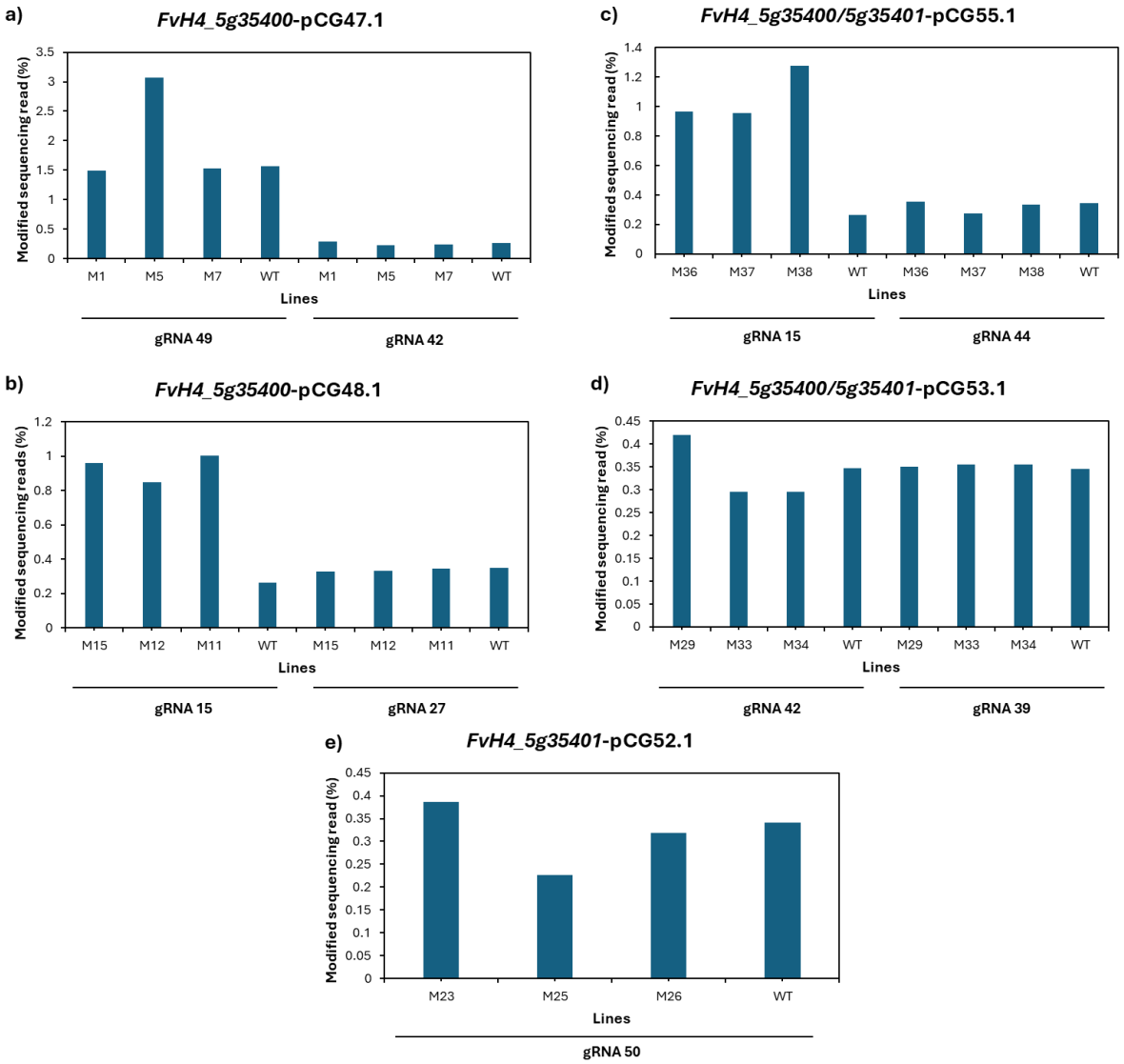

Figure 2. CRISPR/Cas9 mutation analysis of *FvH4_ 5g35400* and *FvH4_ 5g35401* target sites from mutants. Figures show the percentage of modified sequencing reads per sample (mutant line/target site) for: **a)** *FvH4_ 5g35400* (gRNA 49&42); **b)** *FvH4_ 5g35400* (gRNA 15&27); **c)** *FvH4_ 5g35400/FvH_5g35401* (gRNA 15&44); **d)** *FvH4_ 5g35400/FvH_5g35401* (gRNA 42&39); **e)** *FvH4_ 5g35401* (gRNA 50).

Fifteen lines (M1, M5, M7, M11, M12, M15, M23, M25, M26, M29, M33, M34, M36, M37, M38) were selected for amplicon sequencing based on their fragment analysis results. More than

100,000 high quality sequence reads were obtained for each sample. A low proportion of modification reads were obtained across the samples, ranging from 0.2% to 3% **(Figure 2**). The highest number of modified reads (3%) was obtained for *FvH4_5g35400* target site 49 in line M5, followed by line M1 (1.5%) and M7 (1.5%) (**Figure 2a**). Line M38 also showed a comparable percentage of modified read (1.3%) for *FvH4_5g35400* on target site 15 (**Figure 2b**). All the remaining lines presented less than 1% of modified reads (**Figure 2a-e**).

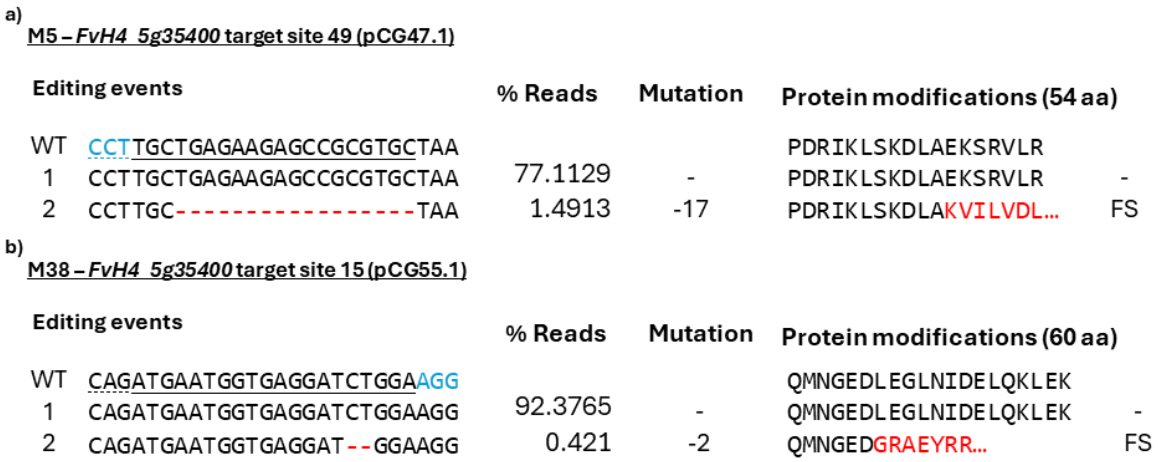

Figure 3. Characterization of CRISPR/Cas9 editing events in selected mutant lines. This figure displays alleles and editing events identified around the target site relative to the wild-type (WT) sequence. **a)** target site 49 from gene *FvH4_5g35400* in mutant line M5; **b)** target site 15 form gene *FvH4_5g35400* in mutant lines M38. gRNA sequence is underlined, the PAM site is shown in blue, and the open reading frame (ORF) is underlined with a dash line. The percentage of sequence reads, type of mutation, and protein modification are shown. Sequence mutations and protein transcoding sequence modifications are indicated in red. FS: Frameshift mutation.

Analysis of target site sequences showed that only lines M5 and M38 presented a detectable editing event in one of the target sites for *FvbH4_5g35400* (**Figure 3**). Line M5 showed a -17 bp deletion in target site 49 detected in 1.5% of the sequencing reads that results in a frameshift (**Figure 3a**). Line M38 presented a -2 bp deletion in target site 15 detected in 0.4% of the sequencing reads that results in a frameshift (**Figure 3b**).

5. Discussion

The global demand for strawberry fruit has steadily increased in recent years and with this the need for year-round availability in the market (Simpson, 2018). This has promoted innovation in cultivation practices and the development of perpetual flowering cultivars for a more consistent supply. The major advantage of perpetual flowering cultivars is that they exhibit a limited response to photoperiod and can flower throughout the growing season, or continuously under controlled conditions (Hancock, 1999). However, one of the major limitations associated with growing perpetual flowering strawberries is the tendency toward low runner production in the generative phase (Darrow, 1919). These limitations stem from the strong physiological trade-off between flowering and runnering, in part due to resource allocation dynamics, by which increased investment in reproductive structures comes at the expense of runner production (Hytönen and Kurokura, 2020; Sønsteby et al., 2021).

Previous studies have investigated the mechanisms controlling flowering and runnering in the diploid woodland strawberry (*Fragaria vesca*), and these highlight the molecular regulation of axillary bud fate as a developmental decision that underpins the trade-off between generative and vegetative growth (Brown, 1965; Caruana et al., 2018; Guttridge and Thompson, 1964; Hytönen et al., 2009; Iwata et al., 2012; Koskela et al., 2012; Rantanen et al., 2015; Lockhart et al., 2017; Tenreira et al., 2017; Andrés et al., 2021; Alonso et al., 2025).

Although *F. vesca* has served as a powerful model for dissecting the molecular pathways underlying these traits, its findings cannot be directly translated to the cultivated strawberry due to the complexity of its octoploid genome and hybrid background (Vondracek et al., 2024; Song et al., 2024; Darby and Islam, 2025). The mechanisms controlling flowering, runnering and the switch between generative and vegetative reproduction in cultivated strawberry (*Fragaria x ananassa*) are yet to be fully understood. Nonetheless, *F. vesca* remains a valuable reference for identifying candidate genes and regulatory networks that may be conserved or functionally relevant in the cultivated strawberry.

Understanding how flowering and runnering are genetically coordinated in *F.* × *ananassa* is essential for addressing the developmental trade-off between generative and vegetative growth. This knowledge is critical for advancing crop improvement approaches, including genome editing, which could be used to modulate the balance between flowering and runnering to ultimately develop elite perpetual flowering cultivars with both optimized yield and sufficient runner production for efficient propagation.

The aim of this work was to investigate the genetic and molecular mechanisms underlying perpetual flowering and continuous runnering in strawberry, with the overall goal of informing crop improvement strategies for both optimized fruit production and vegetative propagation. To achieve this, the experiments described in objective 1 of this thesis study the role of key flowering genes in two cultivated strawberry varieties with contrasting flowering habits (seasonal and perpetual flowering) through genome editing and phenotyping. Objective 2 reports the identification of a major additive QTL for the continuous runnering trait in the woodland strawberry and identifies two major candidate genes associated with this QTL. Objective 3 outlines an attempt to functionally characterize these candidate genes through genome editing.

5.1. Understanding the control of perpetual flowering in strawberry

Understanding the genetic regulation of perpetual flowering in cultivated strawberry remains a challenge. While the genetic and molecular basis of this trait has been well characterized in the woodland strawberry (*F. vesca*), where perpetual flowering arises from a natural loss-of-function mutation in the flowering repressor gene *TFL1*(Koskela et al., 2012), the mechanism in cultivated strawberry is more complex (Darby and Islam, 2025). Historical breeding records and genetic studies have identified three important origins of perpetual flowering in cultivated strawberry: (1) A cultivar from “Gloede’s seedling” originated from France in 1866 (Darrow, 1966); (2) ‘Pan American’, a putative mutant of ‘Bismarck’ selected in New York by S. Cooper in 1898 (Darrow 1966); (3) ‘Wasatch’, a *F. virginiana* subsp. glauca (*S. Watson*) Staudt accession collected in 1955 in the Wasatch Mountains close to Salt Lake City, Utah (Bringhurst and Voth,1980). Although many modern cultivars are descendants of a hybrid between the short-day cultivar ‘Shasta’ and the perpetual flowering ecotype ‘Wasatch’ (Bringhurst and Voth, 1980; Ahmadi et al., 1990; Brukental et al., 2025).

Early studies into the genetic basis of perpetual flowering primarily focused on modern cultivars that include the ‘Wasatch’ linage. Segregation analyses demonstrated that a single dominant locus from ‘Wasatch’ was responsible for the perpetual flowering trait (Bringhurst et al., 1989; Ahmadi et al.,1990). This locus was later mapped as the *PERPETUAL FLOWERING AND RUNNERING* (*FaPFRU*) locus on linkage group IVb-f of the *F. x ananassa* genome (Gaston et al., 2013). The locus was shown to promote flowering while suppressing runnering, indicating a shared regulatory pathway between generative and vegetative reproduction. However, *FaPFRU* is not orthologous to the *F. vesca TFL1* region, further indicating that distinct genetic mechanisms underlie perpetual flowering in woodland and cultivated strawberry. Subsequent studies narrowed down the *FaPFRU* interval and proposed *FT2* as a candidate gene, yet the causal gene(s) remain unknown (Perrotte et al., 2016; Hardigan et al., 2018). Moreover, recent findings showed evidence of the control of

perpetual flowering was more complex, involving the single dominant locus *FaPFRU* and additional epistatic modifier loci (Cockerton et al., 2022).

The difficulty in resolving this regulatory network arises mostly from the polyploid nature of the cultivated strawberry genome, which makes genetic mapping and functional validation of candidate genes difficult (Whitaker et al., 2020; Song et al., 2024). Additionally, the long regeneration time and low transformation efficiency further hinders gene functional studies, making it challenging to understand complex developmental traits such as flowering and runnering (Akter et al., 2024). Despite these limitations, progress has been made in understanding the role of *FaTFL1* (Koskela et al., 2016), largely because of its conserved function as a floral repressor across plant species (Hanano et al., 2011; Kurokura et al., 2013; Kaneko-Suzuki et al., 2018), which makes it a compelling candidate for functional studies aimed at uncovering the genetic basis of perpetual flowering. However, the precise regulatory mechanisms that enable perpetual flowering are yet to be elucidated.

In this context, the experiments in objective 1 focused on narrowing this knowledge gap by building upon functional studies on the roles of key flowering genes *TFL1* and *FT1* in both seasonal and perpetual flowering cultivars. The role of *TFL1* as a floral repressor was supported in the seasonal flowering cultivar Malling Centenary, where mutation in *FaTFL1* resulted in a perpetual flowering phenotype. Moreover, a reduction in runner production was observed in *FaTFL1* mutants, further reinforcing the link between these two traits. However, Koskela et al. (2016) reported contrasting results: while the suppression of *FaTFL1* in the seasonal flowering ‘Elsanta’ cultivar induced perpetual flowering, it did not affect runner production. This variation may reflect genotype specific responses or differences in the degree of *FaTFL1* silencing. While Koskela et al. (2016) achieved a reduction in *FaTFL1* expression through RNAi, the CRISPR/Cas9 approach resulted in partial gene knockout. However, due to known subgenome dominance in the octoploid strawberry genome (Song et al., 2024), it is unclear how much functional *FaTFL1* protein remained. It is possible that the knockout of dominant homoalleles could lead to a stronger phenotypic effect than RNAi silencing, which may only partially reduce expression across all gene copies.

The mutation of *FaFT1* in the perpetual flowering cultivar ‘Calypso’ resulted in alterations in both inflorescence architecture and flower and fruit morphology but did not appear to affect flowering time. These results partially differ from previous findings in *F. vesca*. Koskela et al. (2012) first reported that *FvFT1* acts as a floral activator, promoting flowering under long days, and RNAi silencing of *FvFT1* in the perpetual flowering ‘Hawaii-4’ line led to delayed flowering and reduced expression. This was further validated by Rantanen et al., (2014), who showed that *FvFT1* suppression delayed flowering under different long day light treatments. Kurokura et al. (2017)

further validated this and expanded the understanding of the regulation of *FvFT1* by demonstrating that *FvCO*, a close *CONSTANS* homologue, is required to activate *FvFT1* under long days. More recently, Lembinen et al., (2023) showed that silencing *FvFT1* in 'Hawaii-4' not only affected flower initiation but also had a pronounced impact on inflorescence architecture in *F. vesca*, which aligns with the findings in this study. Taken together, these studies suggest that *FT1* is involved in both flowering time regulation and floral development in strawberry. However, the lack of effect of flowering time observed in the *FaFT1* mutants in this study, highlight a potential functional divergence of *FT1* between woodland and cultivated strawberry. This may be attributed to differences in genetic background or regulatory networks. Although, as discussed previously the partial knockout of this gene could also have a major effect as variations in flowering time were observed between *FaFT1* mutant lines. Although the findings here contribute to the understanding of the molecular control of perpetual flowering in the cultivated strawberry, further functional studies will be needed to understand the precise regulatory mechanisms controlling this trait.

5.2. Dissecting the control of continuous runnering in strawberry

The experiments described in objective 2 and 3 focused on dissecting the developmental switch between flowering and runnering in strawberry. This investigation was driven by the prior identification of the seasonal flowering *F. vesca* accession ES12 from Spain, which maintains active growth and continuous runner production under dormancy inducing short-day conditions. This continuous runnering ecotype thus presents a regional adaptation that enables it to bypass photoperiod induced dormancy and makes it a valuable genetic resource for exploring the mechanisms that regulate axillary bud fate and the transition between vegetative and generative development.

The investigation began by characterizing an F_2 mapping population developed from a cross between the continuous runnering ecotype ES12 and a 'normal' runnering ecotype (ICE12) from Iceland. The significant non-normal distribution of phenotypic traits (runner count, flowering time, leaf count) suggested that this trait may be influenced by a major effect locus, possibly in combination with a polygenic background variation. QTL analysis subsequently identified two additive loci: a major QTL on chromosome Fvb5 explaining over 50% of the phenotypic variation for runner count, flowering time and leaf count during SD treatment; and a minor QTL on chromosome Fvb4 accounting for up to 20% of the variation only for runnering count.

Both QTLs overlap with the previously identified loci associated with branch crown and runner formation by Samad et al. (2017). These loci were identified based on the F_2 population derived from a cross between *F. vesca* perpetual flowering 'Hawaii-4' (H4) and seasonal flowering *F.*

vesca subsp. *vesca* (FV), originally developed by Koskela et al. (2012). In their study they associate the increased number of branch crowns and runners with the 'FV' alleles on both chromosomes. Notably, Samad et al. (2017), reported that the effect of the QTLs on runner production was less pronounced than on branch crown formation, which reflects the genetic background being based on a 'normal' runnering phenotype. In the ES12XICE12 population from this study, the use of a continuous runnering background clearly enhanced the visibility of the runner specific control of these loci and confirmed their role in the regulation of runnering and more specifically axillary bud fate.

Furthermore, the minor QTL identified on chromosome Fvb4 in this study co-localizes with the *FaPFRU* locus previously identified in *F. x ananassa* (Gaston et al., 2013; Perrotte et al., 2016; Saiga et al., 2023). This locus was reported to have a positive effect on flowering and a negative effect on runnering. A recent GWAS study by Brukental et al. (2025), further demonstrated that the *FaPFRU* locus accounted for 22% of the genetic variance in runnering. This aligns with the findings of the study here, where the QTL on Fvb4 showed a relative minor effect for runnering, and supports the assumption that this locus may not be directly regulating runnering in *F. vesca* but presumably influencing axillary bud determination into branch crowns. It is likely that the effect on runnering is an indirect consequence of developmental dynamics: in everbearing genotypes, flowering terminates the primary crown, and subsequent crown development relies on uppermost axillary buds forming new sympodial branches, which themselves terminate in inflorescences (Lembinen et al., (2023).

This repeated pattern limits the number of axillary buds available for runner formation. Moreover, developing flowers and fruits act as strong sink, potentially suppressing runner initiation. This interpretation is supported by Sønsteby et al. (2021), who showed that bi-weekly runner removal in the everbearing cultivar 'Favori' significantly increased fruit yield and size, while leaf thinning had the opposite effect. Their findings highlight that floral initiation and fruit development in everbearing strawberry are source-limited, and that runners compete with floral development. Thus, the observed minor QTL effect on Fvb4 may reflect a shift in axillary bud fate and resource allocation rather than a direct genetic control of runnering.

Candidate genes identified within both QTL include *Dormancy Associated MADS-box* (*DAM*) and *SHORT VEGETATIVE PHASE-like (SVP)* genes, which are primarily associated with flowering time, dormancy and bud outgrowth in plants (Hartmann et al., 2000; Wu et al., 2017; Michaels et al., (2003). Interestingly, expression analysis revealed that one of the DAM genes within the major QTL on Fvb5 (*FvH4_5g35400*) was significantly downregulated in continuous runnering individuals. This gene shares homology with *DAM* genes previously reported in the Evergrowing

peach mutant, which fails to enter dormancy (Bielenberg et al., 2008), and with the *F. x ananassa* gene *FaDAM3* which plays a role in dormancy induction (David et al., 2025a, 2025b). Together, this may suggest a potential role for this gene in dormancy induction, where its repression may bypass dormancy requirement and promote continuous growth and runner production. This would seem to indicate a similar dormancy regulatory mechanism across Rosaceae species. Further functional analysis of the genes identified in objective 2 is necessary to validate their role in the control of dormancy and axillary bud meristem fate in both woodland and cultivated strawberry.

5.3. Study limitations

Despite the potential of CRISPR/Cas9 for functional genomics and crop improvement, its application in polyploid crops such as *F. x ananassa* remains constrained by several biological and technical limitations (Vondracek et al., 2024). One of the primary limitations is the complex nature of its allo-octoploid genome, which comprises four homologous subgenomes and has a high genomic heterozygosity (Hardigan et al., 2021; Han et al., 2022; Song et al., 2024). This introduces both genetic redundancy and allelic variation, making it difficult to design guide RNAs that target all functional gene copies and achieve complete knockouts of target genes (Rodríguez-Leal et al., 2017; Arndell et al., 2019; Hu et al., 2023). Even if one or more alleles are successfully mutated, residual functional copies may mask phenotypic effects, leading to partial or unclear phenotypes (Zaman et al., 2021). This has been clearly reported in Brassica for example, where single-copy mutants show limited phenotypic changes, while simultaneous mutations of multiple homeologs results in a significant phenotypic effect (Ahmar et al., 2022; Ahmad et al., 2023).

Partial editing was one of the major limitations encountered in the work presented in objective 1, as no complete knockout mutant line was obtained. This was evident in the variation of phenotypic outcomes observed among both *FaTFL1* and *FaFT1* mutant lines, where some lines exhibited stronger phenotypes while others closely resembled the wild type. Unusually, this variation did not appear to correlate with the number of edited alleles: in some cases, lines with lower numbers of edited gene copies did exhibit a stronger phenotype. For example, ‘Malling Centenary’ *FaTFL1* mutant line M1, that only presented two edited alleles, flowered earlier than line M6, where four edited alleles were detected. This inconsistency suggests that phenotypic outcome may not simply depend on the number of edited copies, but rather on which subgenome the edits occur in. In this case, M1 carried edits in alleles belonging to subgenome A, which may have a greater functional influence due to subgenome dominance (Edger et al., 2019; Song et al., 2024; Fang et al., 2024). Subgenome A dominance in *F. x ananassa* has been specifically characterized by Song et al., (2024) through comparative transcriptome analysis in the cultivar ‘Benihoppe’. They showed that half of homologous gene pairs were more highly expressed in subgenome A than in B, C and D.

These A-biased genes were involved in developmental processes while B/C/D-biased genes were involved in stress responses and secondary metabolism. Alternatively, the observed variation could also be attributed to the maintenance of functional redundancy among subgenome copies. This has been reported in polyploid species including *Brassica napus* L., where mutations of some specific homoeologs can lead to clear phenotypic changes, while mutations of others may have little to no effect, suggesting differential functional contributions among gene copies (Sirboon et al., 2020; Zaman et al., 2021).

Another potential reason for the discrepancy between number of edited alleles and phenotypic outcome could be off-target editing. The off-target effects occur when Cas9 binds and cleaves untargeted genomic sites that can lead to adverse phenotypic outcomes (Guo et al., 2023). A potential off-target with two mismatches was identified on target site #6 of the *FaTFL1* 'Malling Centenary' mutant line M1. This off-target was located on homologous *CENTRORADIALIS*-like (*CEN*-like)/*TFL1-like* gene in subgenome 3A, 3B and 3C. This gene reportedly plays a crucial role in regulating plant architecture and the transition from vegetative growth to flowering (Amaya et al., 1999; Nakagawa et al., 2002). Therefore, off-target editing in this gene can have an effect in flower initiation in this mutant and could explain the strong phenotypic outcome. Although selecting target sites with off-targets was avoided, some of the targets with the highest predicted efficiency presented several off-targets. In these cases, sequences with off-targets presenting two or more mismatches were selected. However, studies have reported that Cas9 can tolerate several mismatches between the gRNA and the target DNA (Fu et al., 2013; Modrzejewski et al., 2020). Therefore, further screening for off-target editing in mutant lines with predicted off-targets would be required to determine if they have a potential effect on the phenotypic outcomes.

One of the most probable causes of partial knockouts is allelic variation at the target sites which can complicate gRNA design. The presence of multiple homologous gene copies and high heterozygosity in polyploid genomes may result in inefficient gRNA binding due to sequence mismatches between subgenomes or allelic variants. This issue has been addressed in recent genome editing studies in *F. x ananassa* where they have emphasized the importance of sequencing target genes to identify all allelic variants for an efficient gRNA design (Martín-Pizarro et al., 2018; López-Casado et al., 2023). Although sequencing of the target sites was beyond the scope of this study, these findings highlight the importance of considering allelic diversity in future genome editing efforts in *F. x ananassa*. Another alternative reason to partial knockout could be off-target prevalence, as previous studies have shown that CRISPR/Cas9 can cleave off-target sequences with higher efficiency than on-target sites (Corsi et al., 2022).

In this study, CRISPR/Cas9 was specifically used for functional analysis of target genes because of its high specificity and its potential utility in breeding, as it enables stable, heritable gene edits (Lu et al., 2017; Howells et al., 2018; Islam and Kasfy, 2023). Additionally, under some regulatory contexts, CRISPR/Cas9 edited plants are not classified as transgenics and the approach is accepted as a crop improvement technique for the development of commercial varieties (Ahmad et al., 2021; Vondracek et al., 2024). Since the PhD program funding the studies presented here was partly focussed on the potential for commercial exploitation of findings, the use of CRISPR/Cas9 allowed a more 'near market' approach to be tested in this study.

The results from this study further show that using CRISPR for functional mutation in strawberry can be technically challenging. Obtaining complete knockout mutants often requires generating and validating many mutant lines, which can be particularly difficult in strawberry due to its long regeneration period (Cappelletti et al., 2015). This was a challenge that we encountered in the work of both objective 1 and 3 as we obtained a relatively low regeneration and editing efficiency resulting in a small number of transformants to screen. Another limitation experienced was the occurrence of mosaic edits, which potentially resulted in a mixture of editing events within individual lines that may not reliably reflect gene function. This issue particularly affected the progression of the work of objective 3, since the few mutant lines obtained showed a very low percentage of edited cells and therefore have limited value for further phenotypic evaluation.

A more traditional approach for functional validation of genes is RNA interference (RNAi), which relies on post-transcriptional gene silencing and is widely used in plants (Matthew, 2004). One of the major advantages of RNAi is the ability to target genes post-transcriptionally. By acting at the mRNA level, RNAi reduces the need to identify and disrupt all functional gene copies (Malakondaiah et al., 2024). This can be particularly useful in polyploids species like *F. x ananassa* where gene redundancy and subgenome dominance can complicate genome editing approaches. However, one of the disadvantages of using RNAi is that it typically results in partial gene silencing which can lead to variable phenotypic outcomes. Nonetheless, RNAi has been efficiently used in *F. x ananassa* to study key flowering genes including *TFL1* (Koskela et al., 2016). Since this technique can be less technically demanding than CRISPR/Cas9 it remains valuable, potentially for use as a practical first step for functional studies in strawberry.

5.4. Future directions and concluding remarks

This study contributes to the growing understanding of the genetic and molecular regulation of perpetual flowering and runnering in strawberry. The precise regulatory networks controlling these traits remain to be elucidated. However, objective 1 characterized the roles of *TFL1* and *FT1* in

seasonal flowering and perpetual flowering *F. x ananassa* cultivars. *FaTFL1* was validated as a floral repressor, while *FaFT1* was found to influence inflorescence architecture and floral and fruit development. A deeper understanding of the genetic regulation of these key flowering genes is needed to dissect the control of perpetual flowering in strawberry. A central question remaining in this field is whether the *FaPFRU* locus acts upstream of *FaTFL1* potentially repressing its expression or instead acts in parallel by activating flowering independently. Future studies could test this by generating *FaTFL1* knockout lines in a perpetual flowering background and studying the expression of associated flowering genes such as *FaCO*, *FaFT1* and *FaFT2* in both mutant and wild type lines. Additionally, comparative expression profiling of *FaFT1* and *FaTFL1* knockout lines could help clarify the interactions between these genes and their regulation.

To dissect the control of perpetual flowering and continuous runnering, it is important to study the mechanisms regulating the switch from vegetative to generative reproduction, which ultimately involves axillary bud determination. Previous studies have provided some insight into the molecular regulation of axillary bud determination into runners and branch crowns in *F. vesca*. For example, gibberellin (GA) signalling has been found to play a central role in axillary bud determination, particularly in the trade-off between flowering and runnering (Guttridge and Thompson, 1964; Hytönen et al., 2009). Tenreira et al. (2017), showed that *FvGA20ox4*, a gene expressed in axillary meristems that encodes GA20-oxidase enzyme of the GA biosynthesis pathway, was the gene determining the runnerless phenotype in mutant alpine *F.vesca* accessions. Caruana et al. (2018) further demonstrated, in a continuous runnering mutant, that the *FvRGA1* gene, which encodes a DELLA growth repressor, suppresses runner formation when GA levels are low, thereby favouring brand crown development. Furthermore, Alonso et al. (2025) recently identified the *BRANCHED1* (*FvBRC1*) gene as a central regulator of axillary bud determination into branch crowns or runners. Through transcriptome analysis and functional validation, they proposed that *FvBRC1* promotes runner formation by activating the expression *FvGA20ox4*, while also interacting with *FvFT3* florigen to repress runner formation and promote branch crown development.

The work presented in objective 2 provides a new insight into our understanding of the control of axillary bud determination by identifying candidate *DAM* and *SVP-like* genes that potentially play a role in regulating dormancy and axillary bud determination in *F. vesca*. Together with previous studies identifying *FvGA20ox4, FvRGA1* and *FvBRC1* as key regulators of axillary bud determination, these findings contribute to a broader picture of the genetic and hormonal mechanisms controlling the switch between generative and vegetative reproduction in diploid strawberry. To further clarify the regulatory pathways involved, it would be necessary to functionally validate the roles of the candidate genes identified in Chapter 3 and to examine the expression of *FvGA20ox4* and *FvBRC1* in mutants compared to wild type lines. Ultimately these

insights may reveal relevant mechanisms to the control of perpetual flowering and runnering in *F. x ananassa*. To explore this further in *F. x ananassa*, it would be important to study the function and expression of all candidate genes in *FaFT1* and *FaTFL1* mutants in a perpetual flowering cultivar. In conclusion, this research makes an important contribution towards unravelling the molecular networks controlling perpetual flowering and the trade-off between flowering and runnering in strawberry. The development of *FaTFL1* and *FaFT1* edited lines not only clarified their role in regulating flowering and runnering but also demonstrates that CRISPR/Cas9 can be used to modulate key flowering genes to develop novel cultivars. Furthermore, the identification of candidate genes controlling continuous runnering in the woodland strawberry, reveals potential mechanisms involved in the regulation of dormancy and axillary bud determination which can inform crop improvement strategies for the optimization of yield and propagation efficiency in cultivated strawberry.

6. References

Ahmad, A., Munawar, N., Khan, Z., Qusmani, A. T., Khan, S. H., Jamil, A., Ashraf, S., Ghouri, M. Z., Aslam, S., Mubarik, M. S., Munir, A., Sultan, Q., Abd-Elsalam, K. A., & Qari, S. H. (2021). An Outlook on Global Regulatory Landscape for Genome-Edited Crops. *International Journal of Molecular Sciences*, *22*(21), 11753. https://doi.org/10.3390/IJMS222111753

Ahmad, N., Fatima, S., Mehmood, M. A., Zaman, Q. U., Atif, R. M., Zhou, W., Rahman, M. U., & Gill, R. A. (2023). Targeted genome editing in polyploids: lessons from Brassica. *Frontiers in Plant Science*, *14*, 1152468. https://doi.org/10.3389/FPLS.2023.1152468

Ahmadi, H., Bringhurst, R. S., & Voth, V. (1990). Modes of Inheritance of Photoperiodism in Fragaria. *Journal of the American Society for Horticultural Science*, *115*(1), 146–152. https://doi.org/10.21273/JASHS.115.1.146

Ahmar, S., Zhai, Y., Huang, H., Yu, K., Hafeez Ullah Khan, M., Shahid, M., Abdul Samad, R., Ullah Khan, S., Amoo, O., Fan, C., & Zhou, Y. (2022). Development of mutants with varying flowering times by targeted editing of multiple *SVP* gene copies in *Brassica napus* L. The Crop Journal, 10(1), 67–74. https://doi.org/10.1016/J.CJ.2021.03.023

Akter, F., Wu, S., Islam, M. S., Kyaw, H., Yang, J., Li, M., Fu, Y., & Wu, J. (2024). An Efficient Agrobacterium-Mediated Genetic Transformation System for Gene Editing in Strawberry (*Fragaria* × *ananassa*). *Plants*, *13*(5), 563. https://doi.org/10.3390/PLANTS13050563/S1

Alonso, M., Prévost, P., Potier, A., Martin, P. G., Caraglio, Y., Nicolas, M., Hernould, M., Rothan, C., Denoyes, B., & Gaston, A. (2025). Molecular mechanisms underlying the determination of axillary bud fate and outgrowth into branch crown in strawberry. *BioRxiv*, 2025.03.27.645709. https://doi.org/10.1101/2025.03.27.645709

Amaya, I., Ratcliffe, O. J., & Bradley, D. J. (1999). Expression of *CENTRORADIALIS* (*CEN*) and *CEN-like* genes in tobacco reveals a conserved mechanism controlling phase change in diverse species. *The Plant Cell*, *11*(8), 1405. https://doi.org/10.1105/TPC.11.8.1405

Andres, J., Caruana, J., Liang, J., Samad, S., Monfort, A., Liu, Z., Hytonen, T., & Koskela, E. A. (2021). Woodland strawberry axillary bud fate is dictated by a crosstalk of environmental and endogenous factors. *Plant Physiology*, *187*(3), 1221–1234. https://doi.org/10.1093/PLPHYS/KIAB421

Arndell, T., Sharma, N., Langridge, P., Baumann, U., Watson-Haigh, N. S., & Whitford, R. (2019). gRNA validation for wheat genome editing with the CRISPR-Cas9 system. *BMC Biotechnology*, *19*(1), 71. https://doi.org/10.1186/S12896-019-0565-Z

Bielenberg, D. G., Wang, Y., Li, Z., Zhebentyayeva, T., Fan, S., Reighard, G. L., Scorza, R., & Abbott, A. G. (2008). Sequencing and annotation of the evergrowing locus in peach [*Prunus persica* (L.) Batsch] reveals a cluster of six *MADS*-box transcription factors as candidate genes for regulation of terminal bud formation. *Tree Genetics and Genomes*, *4*(3), 495–507. https://doi.org/10.1007/S11295-007-0126-9

Bringhurst, R, and V Voth. (1980). “Six New Strawberry Varieties Released.” *California Agriculture* 34 (2): 12–15.

Bringhurst, R. S., Ahmadi, H., & Voth, V. (1989). Inheritance of the day-neutral trait in strawberries. *Acta Horticulturae*, *265*, 35–42. https://doi.org/10.17660/ACTAHORTIC.1989.265.2

Broman, K. W., Wu, H., Sen, Ś., & Churchill, G. A. (2003). R/qtl: QTL mapping in experimental crosses. *Bioinformatics, 19*(7), 889–890. https://doi.org/10.1093/bioinformatics/btg112

Brown, T., & Wareing, P. F. (1965). The genetical control of the everbearing habit and three other characters in varieties of *Fragaria vesca*. *Euphytica*, *14*(1), 97–112. https://doi.org/10.1007/BF00032819

Brukental, H., Bjornson, M. L., Pincot, D. D. A., Hardigan, M. A., Sharma, S., Jimenez, N. P., Famula, R. A., Ramirez, C. M. L., Cole, G. S., Feldmann, M. J., & Knapp, S. J. (2025). The *PERPETUAL FLOWERING* Locus: Necessary But Insufficient for Genomic Prediction of Runnerless and Other Asexual Reproduction Phenotypes in Strawberry. *BioRxiv*, 2025.04.20.646347. https://doi.org/10.1101/2025.04.20.646347

Cappelletti, R., Sabbadini, S., & Mezzetti, B. (2015). Strawberry (Fragaria × ananassa). *Methods in Molecular Biology (Clifton, N.J.)*, *1224*, 217–227. https://doi.org/10.1007/978-1-4939-1658-0_18

Caruana, J. C., Sittmann, J. W., Wang, W., & Liu, Z. (2018). Suppressor of Runnerless Encodes a DELLA Protein that Controls Runner Formation for Asexual Reproduction in Strawberry. *Molecular Plant*, *11*(1), 230–233. https://doi.org/10.1016/j.molp.2017.11.001

Chen Y., Liu L., Feng Q., Liu C., Bao Y., Zhang N., et al. (2023). *FvWRKY50* is an important gene that regulates both vegetative growth and reproductive growth in strawberry. Hortic. Res. 10, uhad115. 10.1093/hr/uhad115

Corsi, G. I., Qu, K., Alkan, F., Pan, X., Luo, Y., & Gorodkin, J. (2022). CRISPR/Cas9 gRNA activity depends on free energy changes and on the target PAM context. *Nature Communications*, *13*(1), 1–14. https://doi.org/10.1038/S41467-022-30515-0

Darby, E., & Islam, T. (2025). Environmental and molecular regulation of flowering in cultivated strawberry (*Fragaria x ananassa*). *Horticulture Research*, *12*(2). https://doi.org/10.1093/HR/UHAE309

Darrow, G. M. (1919). *Everbearing strawberries*. U.S. Department of Agriculture. Farmers' Bulletin No. 901. https://books.google.com/books/about/Everbearing_Strawberries.html?id=qVzSi458uecC

Darrow, G. M. (1966). The strawberry: History, breeding and physiology. Holt, Rinehart and Winston.

David, S., Han, J., Marcelis, L. F. M., & Verdonk, J. C. (2025). *FaDAM3* and *FaDAM4* are candidate genes for the regulation of seasonal dimorphism in cultivated strawberry. *BioRxiv*, 2024.12.10.627498. https://doi.org/10.1101/2024.12.10.627498

David, S., Kersten, P., Cao, X., Marcelis, L. F. M., & Verdonk, J. C. (2025). *Fragaria ananassa DAM4* expression correlates with vegetative growth during semi-dormancy breaking. *Planta*, *262*(4), 1–15. https://doi.org/10.1007/S00425-025-04799-7

Decaestecker, W., Buono, R. A., Pfeiffer, M. L., Vangheluwe, N., Jourquin, J., Karimi, M., van Isterdael, G., Beeckman, T., Nowack, M. K., & Jacobs, T. B. (2019). CRISPR-Tsko: A technique for efficient mutagenesis in specific cell types, tissues, or organs in *Arabidopsis*. *Plant Cell*, *31*(12), 2868–2887. https://doi.org/10.1105/tpc.19.00454

Diesh, C., Stevens, G. J., Xie, P., de Jesus Martinez, T., Hershberg, E. A., Leung, A., Guo, E., Dider, S., Zhang, J., Bridge, C., Hogue, G., Duncan, A., Morgan, M., Flores, T., Bimber, B. N., Haw, R., Cain, S., Buels, R. M., Stein, L. D., & Holmes, I. H. (2023). JBrowse 2: a modular genome browser with views of synteny and structural variation. *Genome Biology*, *24*(1), 1–21.

Doench, J. G., Hartenian, E., Graham, D. B., Tothova, Z., Hegde, M., Smith, I., Sullender, M., Ebert, B. L., Xavier, R. J., & Root, D. E. (2014). Rational design of highly active sgRNAs for CRISPR-Cas9-mediated gene inactivation. *Nature Biotechnology*, *32*(12), 1262–1267. https://doi.org/10.1038/NBT.3026

Dong, X., Zhang, L. P., Tang, Y. H., Yu, D., Cheng, F., Dong, Y. X., Jiang, X. D., Qian, F. M., Guo, Z. H., & Hu, J. Y. (2023). Arabidopsis *AGAMOUS-LIKE16* and *SUPPRESSOR OF CONSTANS1* regulate the genome-wide expression and flowering time. *Plant Physiology*, *192*(1), 154–169. https://doi.org/10.1093/PLPHYS/KIAD058

Edger, P. P., Poorten, T. J., VanBuren, R., Hardigan, M. A., Colle, M., McKain, M. R., Smith, R. D., Teresi, S. J., Nelson, A. D. L., Wai, C. M., Alger, E. I., Bird, K. A., Yocca, A. E., Pumplin, N., Ou, S., Ben-Zvi, G., Brodt, A., Baruch, K., Swale, T., … Knapp, S. J. (2019). Origin and evolution of the octoploid strawberry genome. *Nature Genetics*, *51*(3), 541–547. https://doi.org/10.1038/S41588-019-0356-4

Elshire, R. J., Glaubitz, J. C., Sun, Q., Poland, J. A., Kawamoto, K., Buckler, E. S., & Mitchell, S. E. (2011). A robust, simple genotyping-by-sequencing (GBS) approach for high diversity species. *PLoS ONE*, *6*(5). https://doi.org/10.1371/journal.pone.0019379

Engler, C., & Marillonnet, S. (2014). Golden Gate cloning. *Methods in Molecular Biology*, *1116*, 119–131. https://doi.org/10.1007/978-1-62703-764-8_9

Fang, C., Jiang, N., Teresi, S. J., Platts, A. E., Agarwal, G., Niederhuth, C., Edger, P. P., & Jiang, J. (2024). Dynamics of accessible chromatin regions and subgenome dominance in octoploid strawberry. *Nature Communications*, *15*(1). https://doi.org/10.1038/S41467-024-46861-0

Fu, Y., Foden, J. A., Khayter, C., Maeder, M. L., Reyon, D., Joung, J. K., & Sander, J. D. (2013). High-frequency off-target mutagenesis induced by CRISPR-Cas nucleases in human cells. *Nature Biotechnology*, *31*(9), 822–826. https://doi.org/10.1038/NBT.2623

Gaston, A., Perrotte, J., Lerceteau-Köhler, E., Rousseau-Gueutin, M., Petit, A., Hernould, M., Rothan, C., & Denoyes, B. (2013). *PFRU*, a single dominant locus regulates the balance between

sexual and asexual plant reproduction in cultivated strawberry. *Journal of Experimental Botany*, *64*(7), 1837–1848. https://doi.org/10.1093/JXB/ERT047

Greb, T., Mylne, J. S., Crevillen, P., Geraldo, N., An, H., Gendall, A. R., & Dean, C. (2007). The PHD Finger Protein *VRN5* Functions in the Epigenetic Silencing of Arabidopsis *FLC*. *Current Biology*, *17*(1), 73–78. https://doi.org/10.1016/j.cub.2006.11.052

Guo, C., Ma, X., Gao, F., & Guo, Y. (2023). Off-target effects in CRISPR/Cas9 gene editing. *Frontiers in Bioengineering and Biotechnology*, *11*, 1143157. https://doi.org/10.3389/FBIOE.2023.1143157

Guttridge, C. G., & Thompson, P. A. (1964). The Effect of Gibberellins on Growth and Flowering of *Fragaria* and *Duchesnea*. *Journal of Experimental Botany*, *15*(3), 631–646. https://doi.org/10.1093/JXB/15.3.631

Haeussler, M., Schönig, K., Eckert, H., Eschstruth, A., Mianne, J., Renaud, J.B., Schneider-Maunoury, S., Shkumatava, A., Teboul, L., Kent, J., Joly, J.S. and Concordet, J.P. (2016). CRISPOR: intuitive guide selection for CRISPR/Cas9 genome editing experiments. *Nucleic Acids Research*, 44(W1), W242-W247. https://doi.org/10.1093/nar/gkw442

Han, H., Barbey, C. R., Fan, Z., Verma, S., Whitaker, V. M., & Lee, S. (2022). Telomere-to-Telomere and Haplotype-Phased Genome Assemblies of the Heterozygous Octoploid 'Florida Brilliance' Strawberry (*Fragaria* × *ananassa*). *BioRxiv*, 2022.10.05.509768. https://doi.org/10.1101/2022.10.05.509768

Hanano, S., & Goto, K. (2011). Arabidopsis *TERMINAL FLOWER1* Is Involved in the Regulation of Flowering Time and Inflorescence Development through Transcriptional Repression. *The Plant Cell*, *23*(9), 3172–3184. https://doi.org/10.1105/TPC.111.088641

Hancock, James. F. (1999). Strawberries (1st ed.). CABI Publishing.

Hardigan, M. A., Lorant, A., Pincot, D. D. A., Feldmann, M. J., Famula, R. A., Acharya, C. B., Lee, S., Verma, S., Whitaker, V. M., Bassil, N., Zurn, J., Cole, G. S., Bird, K., Edger, P. P., & Knapp, S. J. (2021). Unraveling the Complex Hybrid Ancestry and Domestication History of Cultivated Strawberry. *Molecular Biology and Evolution*, *38*(6), 2285–2305. https://doi.org/10.1093/MOLBEV/MSAB024

Hardigan, M. A., Poorten, T. J., Acharya, C. B., Cole, G. S., Hummer, K. E., Bassil, N., Edger, P. P., & Knapp, S. J. (2018). Domestication of Temperate and Coastal Hybrids with Distinct Ancestral Gene Selection in Octoploid Strawberry. *The Plant Genome*, *11*(3), 180049. https://doi.org/10.3835/PLANTGENOME2018.07.0049

Hartmann, U., Höhmann, S., Nettesheim, K., Wisman, E., Saedler, H., & Huijser, P. (2000). Molecular cloning of *SVP*: a negative regulator of the floral transition in *Arabidopsis*. *The Plant Journal*, *21*(4), 351–360. https://doi.org/10.1046/J.1365-313X.2000.00682.X

Howells, R. M., Craze, M., Bowden, S., & Wallington, E. J. (2018). Efficient generation of stable, heritable gene edits in wheat using CRISPR/Cas9. *BMC Plant Biology*, *18*(1), 1–11. https://doi.org/10.1186/S12870-018-1433-Z

Hu, Y., Patra, P., Pisanty, O., Shafir, A., Belew, Z. M., Binenbaum, J., ben Yaakov, S., Shi, B., Charrier, L., Hyams, G., Zhang, Y., Trabulsky, M., Caldararu, O., Weiss, D., Crocoll, C., Avni, A., Vernoux, T., Geisler, M., Nour-Eldin, H. H., … Shani, E. (2023). Multi-Knock – a multi-targeted genome-scale CRISPR toolbox to overcome functional redundancy in plants. *Nature Plants*, *9*(4), 572. https://doi.org/10.1038/S41477-023-01374-4

Hytönen, T., & Kurokura, T. (2020). Control of flowering and runnering in strawberry. In *Horticulture Journal* (Vol. 89, Issue 2, pp. 96–107). Japanese Society for Horticultural Science. https://doi.org/10.2503/hortj.UTD-R011

Hytönen, T., Elomaa, P., Moritz, T., & Junttila, O. (2009). Gibberellin mediates daylength-controlled differentiation of vegetative meristems in strawberry (*Fragaria* × *ananassa* Duch). *BMC Plant Biology*, *9*(1), 1–12. https://doi.org/10.1186/1471-2229-9-18

Islam, T., & Kasfy, S. H. (2023). CRISPR enables heritable genome editing in planta. *Trends in Genetics*, *39*(9), 646–648. https://doi.org/10.1016/J.TIG.2023.06.009

Iwata, H., Gaston, A., Remay, A., Thouroude, T., Jeauffre, J., Kawamura, K., Oyant, L. H. saint, Araki, T., Denoyes, B., & Foucher, F. (2012). The *TFL1* homologue *KSN* is a regulator of continuous flowering in rose and strawberry. *The Plant Journal*, *69*(1), 116–125. https://doi.org/10.1111/J.1365-313X.2011.04776.X

Jung, S., Lee, T., Cheng, C. H., Buble, K., Zheng, P., Yu, J., Humann, J., Ficklin, S. P., Gasic, K., Scott, K., Frank, M., Ru, S., Hough, H., Evans, K., Peace, C., Olmstead, M., DeVetter, L. W., McFerson, J., Coe, M., Wegrzyn, J.L., Staton, M.E., Abbott, A.G., & Main, D. (2019). 15 years of GDR: New data and functionality in the Genome Database for Rosaceae. *Nucleic Acids Research*, *47*(D1), D1137–D1145. https://doi.org/10.1093/nar/gky1000

Kaneko-Suzuki, M., Kurihara-Ishikawa, R., Okushita-Terakawa, C., Kojima, C., Nagano-Fujiwara, M., Ohki, I., Tsuji, H., Shimamoto, K., & Taoka, K. I. (2018). *TFL1-Like* Proteins in Rice Antagonize Rice *FT-Like* Protein in Inflorescence Development by Competition for Complex Formation with 14-3-3 and FD. *Plant and Cell Physiology*, *59*(3), 458–468. https://doi.org/10.1093/PCP/PCY021
Kieffer, M., Master, V., Waites, R., & Davies, B. (2011). *TCP14* and *TCP15* affect internode length and leaf shape in Arabidopsis. *The Plant Journal*, *68*(1), 147–158. https://doi.org/10.1111/J.1365-313X.2011.04674.X

Kim, K., Lee, J., Kim, B., Shin, J., Kang, T. A., & Kim, W. C. (2022). *GATA25*, a novel regulator, accelerates the flowering time of *Arabidopsis thaliana*. *Applied Biological Chemistry*, *65*(1), 1–8. https://doi.org/10.1186/s13765-022-00698-7

Koskela, E. A., Mouhu, K., Albani, M. C., Kurokura, T., Rantanen, M., Sargent, D. J., Battey, N. H., Coupland, G., Elomaa, P., & Hytönen, T. (2012). Mutation in *TERMINAL FLOWER1* Reverses the Photoperiodic Requirement for Flowering in the Wild Strawberry *Fragaria vesca*. *Plant Physiology*, *159*(3), 1043. https://doi.org/10.1104/PP.112.196659

Koskela, E. A., Sønsteby, A., Flachowsky, H., Heide, O. M., Hanke, M. V., Elomaa, P., & Hytönen, T. (2016). *TERMINAL FLOWER1* is a breeding target for a novel everbearing trait and tailored flowering responses in cultivated strawberry (*Fragaria* × *ananassa* Duch.). Plant Biotechnology Journal, 14(9), 1852–1861. https://doi.org/10.1111/PBI.12545

Kurokura, T., Mimida, N., Battey, N. H., & Hytönen, T. (2013). The regulation of seasonal flowering in the Rosaceae. *Journal of Experimental Botany*, *64*(14), 4131–4141. https://doi.org/10.1093/JXB/ERT233

Kurokura, T., Samad, S., Koskela, E., Mouhu, K., & Hytönen, T. (2017). *Fragaria vesca CONSTANS* controls photoperiodic flowering and vegetative development. *Journal of Experimental Botany*, *68*(17), 4839–4850. https://doi.org/10.1093/JXB/ERX301

Labun, K., Montague, T. G., Krause, M., Torres Cleuren, Y. N., Tjeldnes, H., & Valen, E. (2019). CHOPCHOP v3: expanding the CRISPR web toolbox beyond genome editing. *Nucleic Acids Research*, *47*(W1), W171–W174. https://doi.org/10.1093/NAR/GKZ365

Lembinen, S., Cieslak, M., Zhang, T., Mackenzie, K., Elomaa, P., Prusinkiewicz, P., & Hytönen, T. (2023). Diversity of woodland strawberry inflorescences arises from heterochrony regulated by *TERMINAL FLOWER 1* and *FLOWERING LOCUS T*. *The Plant Cell*, *35*(6), 2079–2094. https://doi.org/10.1093/PLCELL/KOAD086

Lockhart, J. (2017). Flowering Versus Runnering: Uncovering the Protein Behind a Trait That Matters in Strawberry. *The Plant Cell*, *29*(9), 2080–2081. https://doi.org/10.1105/TPC.17.00709

López-Casado, G., Sánchez-Raya, C., Ric-Varas, P. D., Paniagua, C., Blanco-Portales, R., Muñoz-Blanco, J., Pose, S., Matas, A. J., & Mercado, J. A. (2023). CRISPR/Cas9 editing of the polygalacturonase *FaPG1* gene improves strawberry fruit firmness. *Horticulture Research*, *10*(3), uhad011. https://doi.org/10.1093/HR/UHAD011

Lu, Y., Ye, X., Guo, R., Huang, J., Wang, W., Tang, J., Tan, L., Zhu, J. kang, Chu, C., & Qian, Y. (2017). Genome-wide Targeted Mutagenesis in Rice Using the CRISPR/Cas9 System. Molecular Plant, 10(9), 1242–1245. https://doi.org/10.1016/j.molp.2017.06.007

Malakondaiah, S., Julius, A., Ponnambalam, D., Gunthoti, S. S., Ashok, J., Krishana, P. S., & Rebecca, J. (2024). Gene silencing by RNA interference: a review. *Genome Instability & Disease 2024 5:5*, *5*(5), 225–241. https://doi.org/10.1007/S42764-024-00135-7

Martín-Pizarro, C., Triviño, J. C., & Posé, D. (2018). Functional analysis of the *TM6 MADS-box* gene in the octoploid strawberry by CRISPR/Cas9-directed mutagenesis. *Journal of Experimental Botany*, *70*(3), 885. https://doi.org/10.1093/JXB/ERY400

Matthew, L. (2004). RNAi for Plant Functional Genomics. *Comparative and Functional Genomics*, *5*(3), 240. https://doi.org/10.1002/CFG.396

Michaels, S. D., Ditta, G., Gustafson-Brown, C., Pelaz, S., Yanofsky, M., & Amasino, R. M. (2003). *AGL24* acts as a promoter of flowering in *Arabidopsis* and is positively regulated by vernalization. *The Plant Journal*, *33*(5), 867–874. https://doi.org/10.1046/J.1365-313X.2003.01671.X

Modrzejewski, D., Hartung, F., Lehnert, H., Sprink, T., Kohl, C., Keilwagen, J., & Wilhelm, R. (2020). Which Factors Affect the Occurrence of Off-Target Effects Caused by the Use of CRISPR/Cas: A Systematic Review in Plants. *Frontiers in Plant Science*, *11*, 574959. https://doi.org/10.3389/FPLS.2020.574959

Mouhu, K., Kurokura, T., Koskela, E. A., Albert, V. A., Elomaa, P., & Hytönen, T. (2013). The *Fragaria vesca* Homolog of *SUPPRESSOR OF OVEREXPRESSION OF CONSTANS1* Represses Flowering and Promotes Vegetative Growth. *The Plant Cell*, *25*(9), 3296–3310. https://doi.org/10.1105/TPC.113.115055

Nakagawa, M., Shimamoto, K., & Kyozuka, J. (2002). Overexpression of *RCN1* and *RCN2*, rice *TERMINAL FLOWER 1/CENTRORADIALIS* homologs, confers delay of phase transition and altered panicle morphology in rice. *The Plant Journal : For Cell and Molecular Biology*, *29*(6), 743–750. https://doi.org/10.1046/J.1365-313X.2002.01255.X

Nicoli, M. F., & Galletta, G. J. (1987). Variation in Growth and Flowering Habits of Junebearing and Everbearing Strawberries. *Journal of the American Society for Horticultural Science*, *112*(5), 872–880. https://doi.org/10.21273/JASHS.112.5.872

Perrotte, J., Gaston, A., Potier, A., Petit, A., Rothan, C., & Denoyes, B. (2016). Narrowing down the single homoeologous *FaPFRU* locus controlling flowering in cultivated octoploid strawberry using a selective mapping strategy. *Plant Biotechnology Journal*, *14*(11), 2176–2189. https://doi.org/10.1111/PBI.12574;JOURNAL:JOURNAL:14677652;WGROUP:STRING:PUBLICATION

Rantanen, M., Kurokura, T., Jiang, P., Mouhu, K., & Hytönen, T. (2015). Strawberry homologue of *TERMINAL FLOWER1* integrates photoperiod and temperature signals to inhibit flowering. *The Plant Journal*, *82*(1), 163–173. https://doi.org/10.1111/TPJ.12809

Rodríguez-Leal, D., Lemmon, Z. H., Man, J., Bartlett, M. E., & Lippman, Z. B. (2017). Engineering Quantitative Trait Variation for Crop Improvement by Genome Editing. *Cell*, *171*(2), 470-480.e8. https://doi.org/10.1016/j.cell.2017.08.030

Ruiz-Rojas, J.J., Sargent, D.J., Shulaev, V., Dickerman, A.W., Pattison, J., Holt, S.H., Ciordia, A., and Veilleux, R.E. (2010). SNP discovery and genetic mapping of T-DNA insertional mutants in *Fragaria vesca* L. *Theor. Appl. Genet.* 121: 449–463. https://doi.org/10.1007/s00122-010-1322-9
Samad, S., Kurokura, T., Koskela, E., Toivainen, T., Patel, V., Mouhu, K., Sargent, D. J., & Hytönen, T. (2017). Additive QTLs on three chromosomes control flowering time in woodland strawberry (*Fragaria vesca* L.). *Horticulture Research*, *4*(1), 1–11. https://doi.org/10.1038/HORTRES.2017.20

Sargent, D. J., Hadonou, A. M., & Simpson, D. W. (2003). Development and characterization of polymorphic microsatellite markers from *Fragaria viridis*, a wild diploid strawberry. *Molecular Ecology Notes*, *3*(4), 550–552. https://doi.org/10.1046/J.1471-8286.2003.00507.X

Shulaev, V., Sargent, D. J., Crowhurst, R. N., Mockler, T. C., Folkerts, O., Delcher, A. L., Jaiswal, P., Mockaitis, K., Liston, A., Mane, S. P., Burns, P., Davis, T. M., Slovin, J. P., Bassil, N., Hellens, R. P., Evans, C., Harkins, T., Kodira, C., Desany, B., … Folta, K. M. (2011). The genome of

woodland strawberry (*Fragaria vesca*). *Nature Genetics*, *43*(2), 109–116. https://doi.org/10.1038/NG.740

Simpson, D. (2018). *The Economic Importance of Strawberry Crops*. 1–7. https://doi.org/10.1007/978-3-319-76020-9_1

Song, Y., Peng, Y., Liu, L., Li, G., Zhao, X., Wang, X., Cao, S., Muyle, A., Zhou, Y., & Zhou, H. (2024). Phased gap-free genome assembly of octoploid cultivated strawberry illustrates the genetic and epigenetic divergence among subgenomes. *Horticulture Research*, *11*(1). https://doi.org/10.1093/HR/UHAD252

Sønsteby, A., Woznicki, T. L., & Heide, O. M. (2021). Effects of Runner Removal and Partial Defoliation on the Growth and Yield Performance of 'Favori' Everbearing Strawberry Plants. *Horticulturae 2021, Vol. 7, Page 215*, *7*(8), 215. https://doi.org/10.3390/HORTICULTURAE7080215

Sriboon, S., Li, H., Guo, C., Senkhamwong, T., Dai, C., & Liu, K. (2020). Knock-out of *TERMINAL FLOWER 1* genes altered flowering time and plant architecture in *Brassica napus*. *BMC Genetics*, *21*(1), 1–13. https://doi.org/10.1186/S12863-020-00857-Z

Sung, S., & Amasino, R. M. (2004). Vernalization in Arabidopsis thaliana is mediated by the PHD finger protein *VIN3*. *Nature*, *427*(6970), 159–164. https://doi.org/10.1038/NATURE02195
Tenreira, T., Pimenta Lange, M. J., Lange, T., Bres, C., Labadie, M., Monfort, A., Hernould, M., Rothan, C., & Denoyes, B. (2017). A Specific Gibberellin 20-Oxidase Dictates the Flowering-Runnering Decision in Diploid Strawberry. *The Plant Cell*, *29*(9), 2168–2182. https://doi.org/10.1105/TPC.16.00949

Tenreira, T., Pimenta Lange, M. J., Lange, T., Bres, C., Labadie, M., Monfort, A., Hernould, M., Rothan, C., & Denoyes, B. (2017). A Specific Gibberellin 20-Oxidase Dictates the Flowering-Runnering Decision in Diploid Strawberry. *The Plant Cell*, *29*(9), 2168–2182. https://doi.org/10.1105/TPC.16.00949

Van Ooijen, J.W. (2004). MapQTL 5: Software for the mapping of quantitative trait loci in experimental populations. *Kyazma B.V., Wageningen*. Online: www.kyazma.nl

Vondracek, K., Altpeter, F., Liu, T., & Lee, S. (2024). Advances in genomics and genome editing for improving strawberry (*Fragaria ×ananassa*). *Frontiers in Genetics*, *15*, 1382445. https://doi.org/10.3389/FGENE.2024.1382445

Wei, W., Hu, Y., Cui, M. Y., Han, Y. T., Gao, K., & Feng, J. Y. (2016). Identification and transcript analysis of the TCP transcription factors in the diploid woodland strawberry *Fragaria vesca*. *Frontiers in Plant Science*, 229140. https://doi.org/10.3389/FPLS.2016.01937

Whitaker, V. M., Knapp, S. J., Hardigan, M. A., Edger, P. P., Slovin, J. P., Bassil, N. v., Hytönen, T., Mackenzie, K. K., Lee, S., Jung, S., Main, D., Barbey, C. R., & Verma, S. (2020). A roadmap for research in octoploid strawberry. *Horticulture Research*, *7*(1), 33. https://doi.org/10.1038/S41438-020-0252-1

Wilson, F. M., Harrison, K., Armitage, A. D., Simkin, A. J., & Harrison, R. J. (2019). CRISPR/Cas9-mediated mutagenesis of phytoene desaturase in diploid and octoploid strawberry. *Plant Methods*, *15*(1). https://doi.org/10.1186/s13007-019-0428-6

Wu, R., Tomes, S., Karunairetnam, S., Tustin, S. D., Hellens, R. P., Allan, A. C., Macknight, R. C., & Varkonyi-Gasic, E. (2017). *SVP-Like MADS* box genes control dormancy and budbreak in apple. *Frontiers in Plant Science*, *8*, 256625. https://doi.org/10.3389/FPLS.2017.00477

Zaman, Q. U., Wen, C., Yuqin, S., Mengyu, H., Desheng, M., Jacqueline, B., Baohong, Z., Chao, L., & Qiong, H. (2021). Characterization of *SHATTERPROOF* Homoeologs and CRISPR-Cas9-Mediated Genome Editing Enhances Pod-Shattering Resistance in *Brassica napus* L. *CRISPR Journal*, *4*(3), 360–370. https://doi.org/10.1089/CRISPR.2020.0129